

QCD and Its Success



Rutherford Scattering

Rutherford taught us the most important lesson:
use a **scattering process** to learn about the structure of matter

This story is well known:

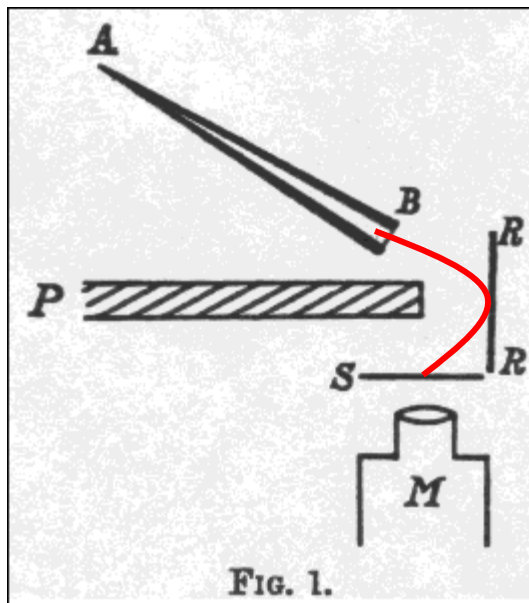
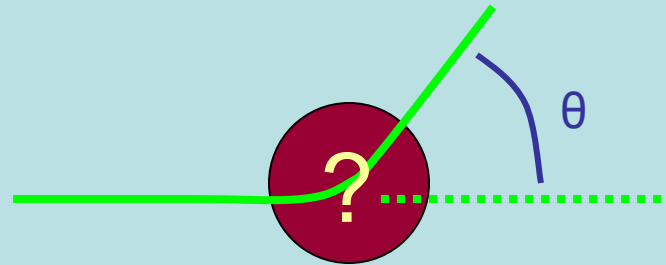
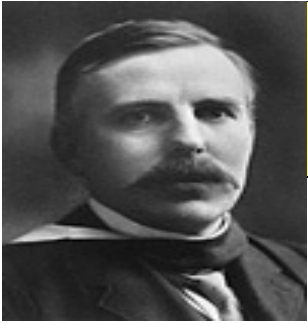


FIG. 1.

H. Geiger and E. Marsden observed that α -particles were sometimes scattered through very large angles.

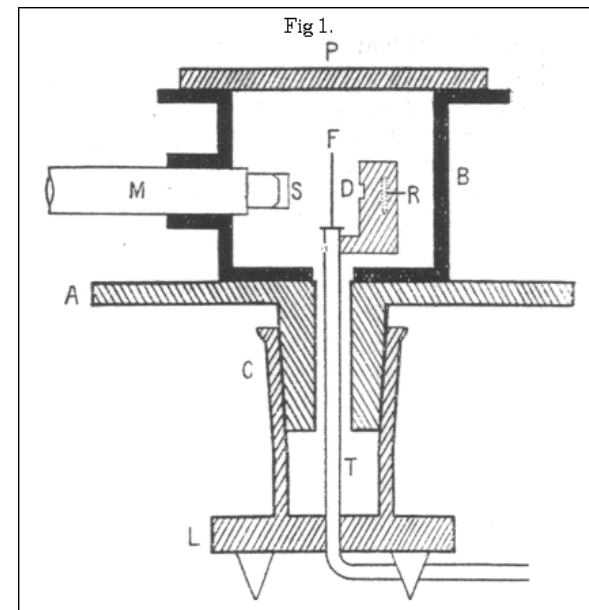
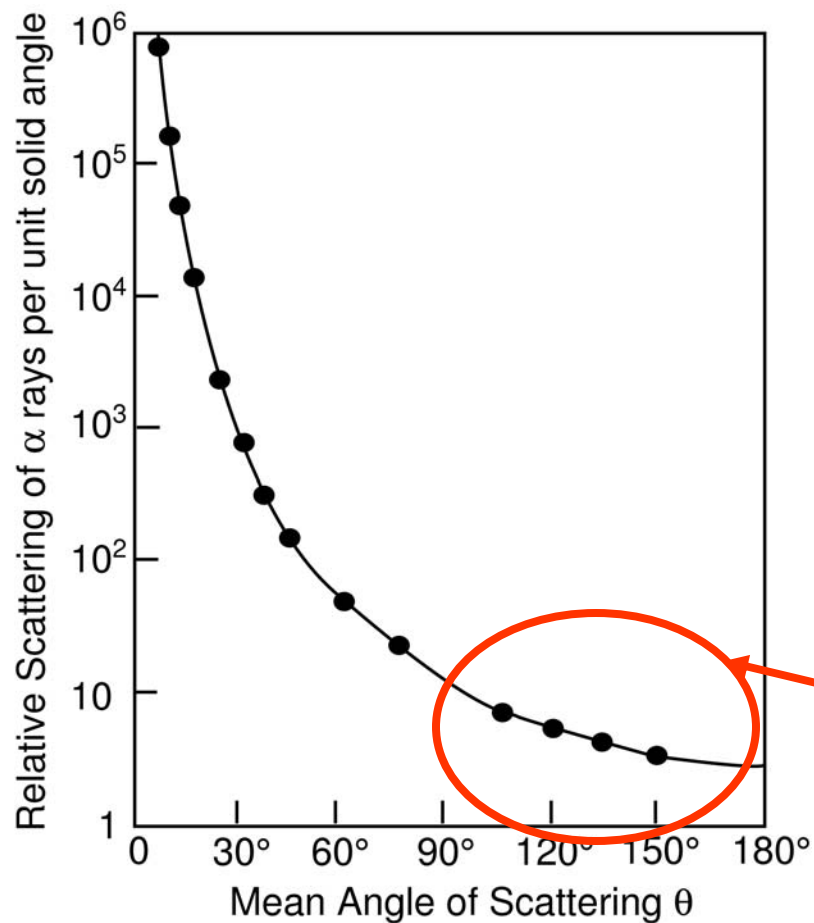
Rutherford interpreted these results as due to the coulomb scattering of the α -particles with the **atomic nucleus**:

$$\sigma(\theta) = \frac{z^2 Z^2 e^4}{16E^2} \frac{1}{\sin^4 \frac{1}{2}\theta}$$



Rutherford Scattering

In a subsequent paper Geiger/Marsden precisely verified Rutherford theory



Discovery of atomic nucleus

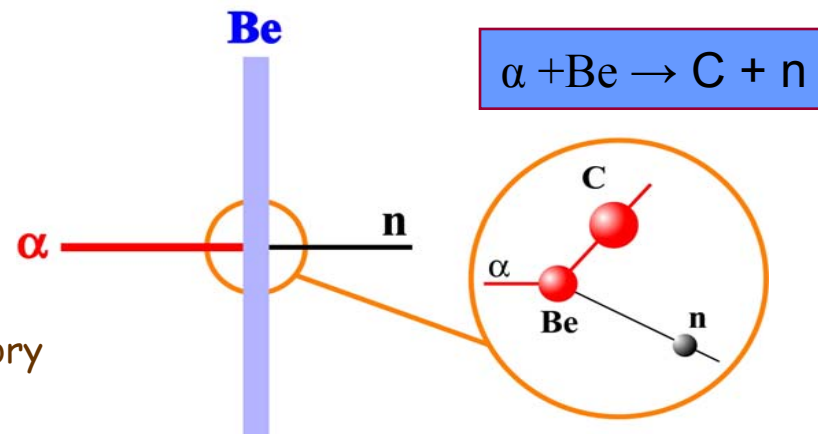
→ N. Bohr Old Quantum theory...

Developments...

- Quantum mechanics rapidly developed in the years 1924-27
- The nucleus composition remained a mystery (e.g. N_7^{14}) till...

Discovery of neutron (Chadwick 1932)

Instrumental to the Fermi's beta decay ($n \rightarrow p + e + \bar{\nu}$) theory



Main information concerning geometric details of nuclear structure (mirror nuclei, fast neutron capture, binding energies etc) could be summed up in:

$$R = r_0 \times A^{1/3} \text{ fm} \quad \text{with } r_0 = 1.45 \text{ fm}$$

$$\rho_m = 0.08 \text{ nucl}/\text{fm}^3 \quad \text{and} \quad \rho_c = (Z/A) \times 0.08 \text{ (prot. charges)}/\text{fm}^3$$

The nucleus form factor

Stimulated by **accelerators technology advances** and **fully mature QED** various theoreticians (Rose (48), Elton(50)) started to calculate cross sections for elastic electron-Nucleus scattering

$$\sigma_M(\theta) = \left(\frac{Ze^2}{2E}\right)^2 \frac{\cos^2 \frac{1}{2}\theta}{\sin^4 \frac{1}{2}\theta} \quad \text{Mott}$$

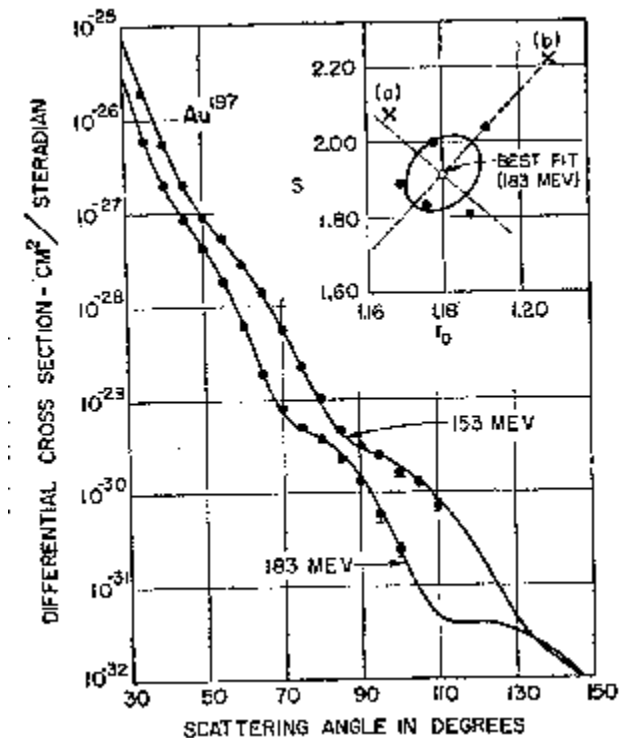
$$\sigma_s(\theta) = \left(\frac{Ze^2}{2E}\right)^2 \frac{\cos^2 \frac{1}{2}\theta}{\sin^4 \frac{1}{2}\theta} \left| \int_{\text{nuclear volume}} \rho(r) e^{i\mathbf{q} \cdot \mathbf{r}} d\tau \right|^2$$

$$\sigma_s(\theta) = \left(\frac{Ze^2}{2E}\right)^2 \frac{\cos^2 \frac{1}{2}\theta}{\sin^4 \frac{1}{2}\theta} \left[\int_0^\infty \rho(r) \frac{\sin qr}{qr} 4\pi r^2 dr \right]^2$$

$$F = \frac{4\pi}{q} \int_0^\infty \rho(r) \sin(qr) r dr$$

Nucleus form factor

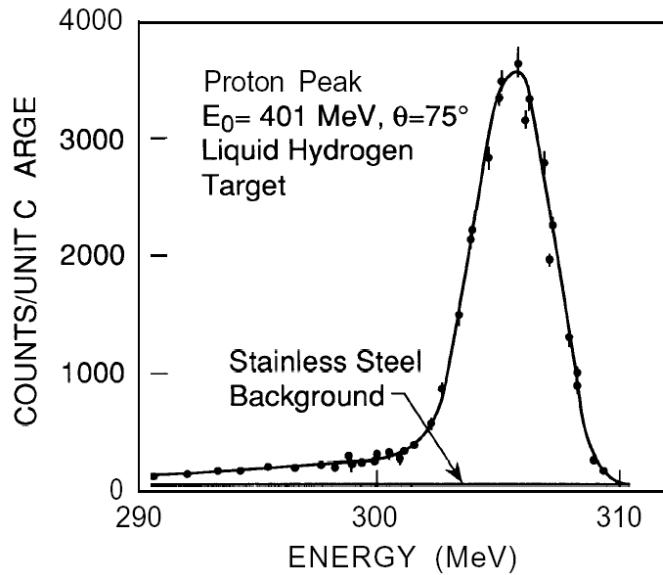
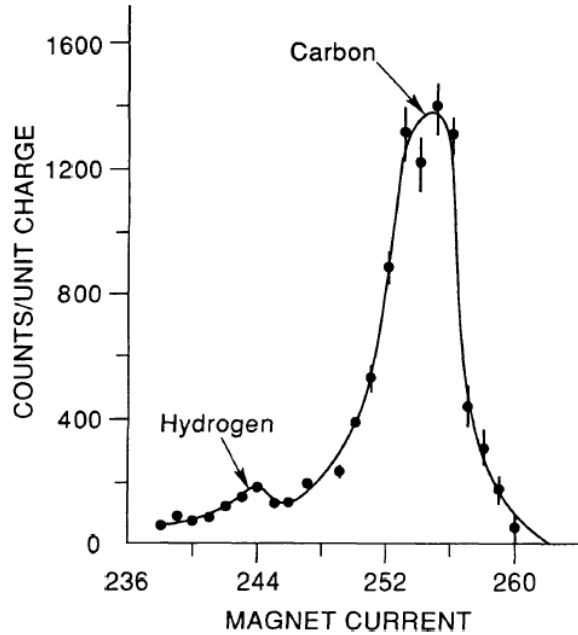
Interference between the scattered wavelets arising from the different parts of the same, finite, nucleus



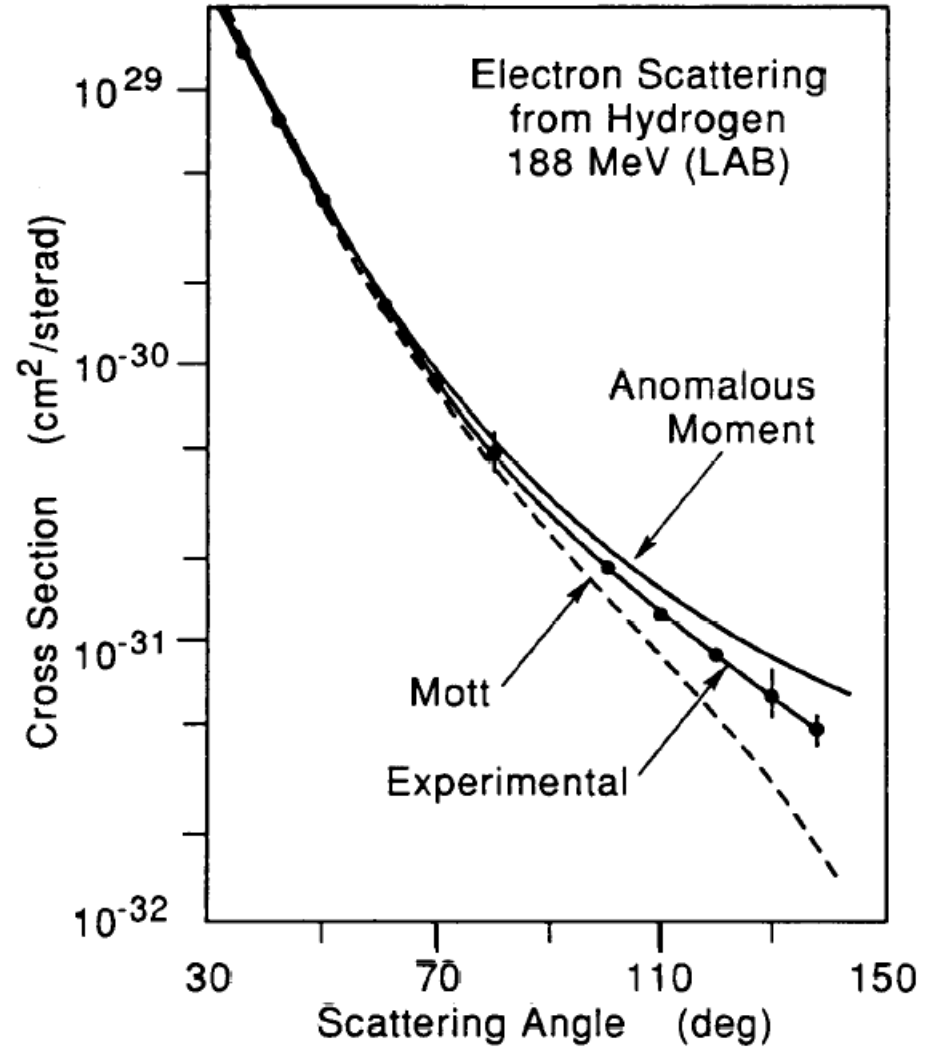
Phase-shift analysis



R. Hofstadter: e-p elastic scattering



$$\frac{d\sigma}{d\Omega} = \frac{a^2}{4E_0^2 \sin^4 \theta/2} \cdot \cos^2 \theta/2 \cdot \frac{E'}{E_0} \left[\frac{G_E^2 + \tau G_M^2}{1 + \tau} + 2\tau G_M^2 \tan^2 \theta/2 \right]$$



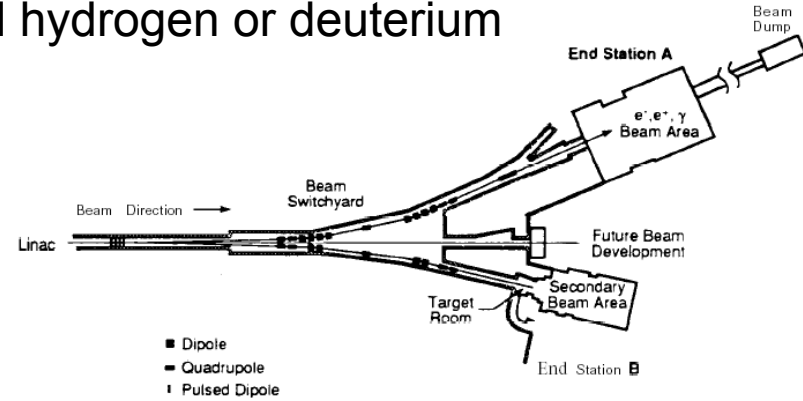
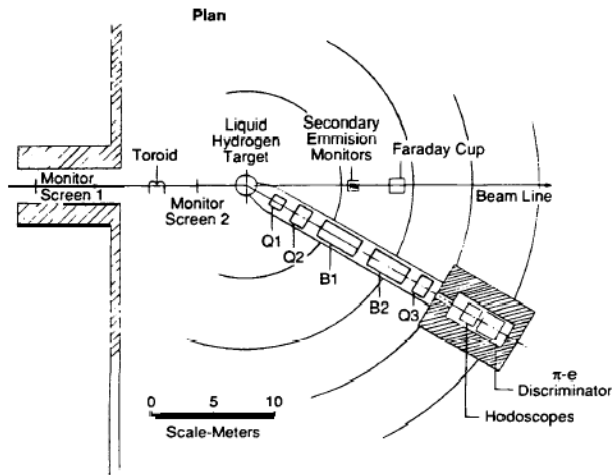
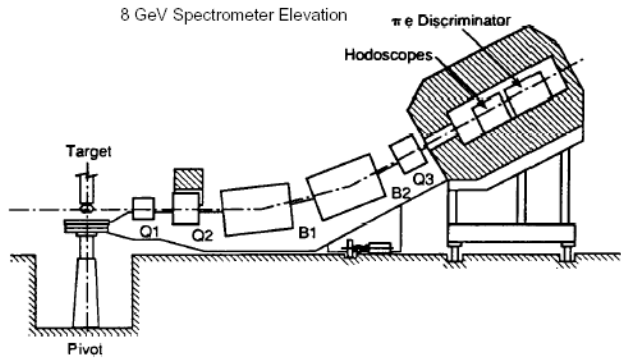


1990 Nobel Prize

The SLAC-MIT Experiment

Under the leadership of Taylor, Friedman, Kendall
 ~ 1969

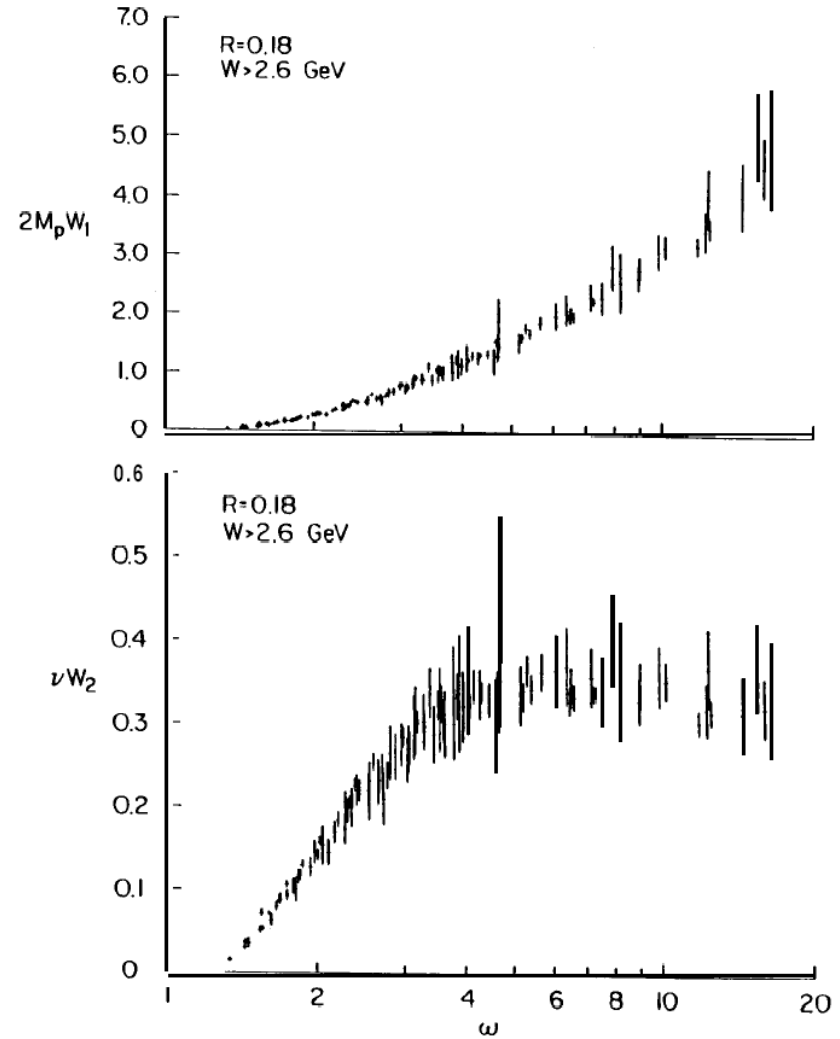
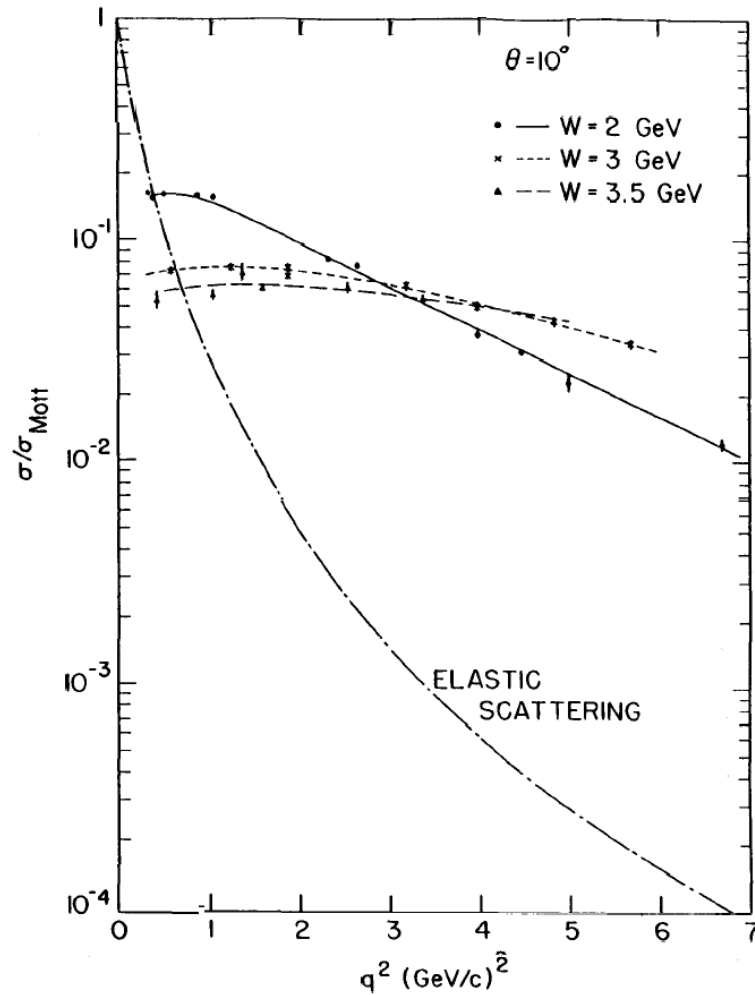
Electron scattered by
 liquid hydrogen or deuterium



First SLAC-MIT results

Two unexpected results...

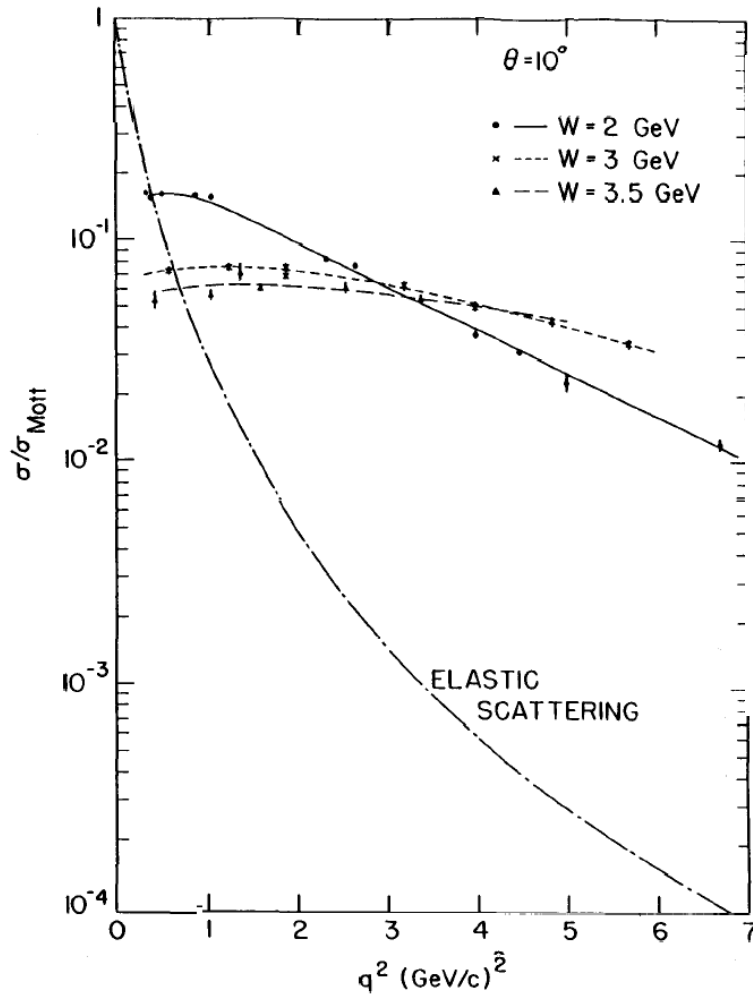
Deep-inelastic scattering (DIS)



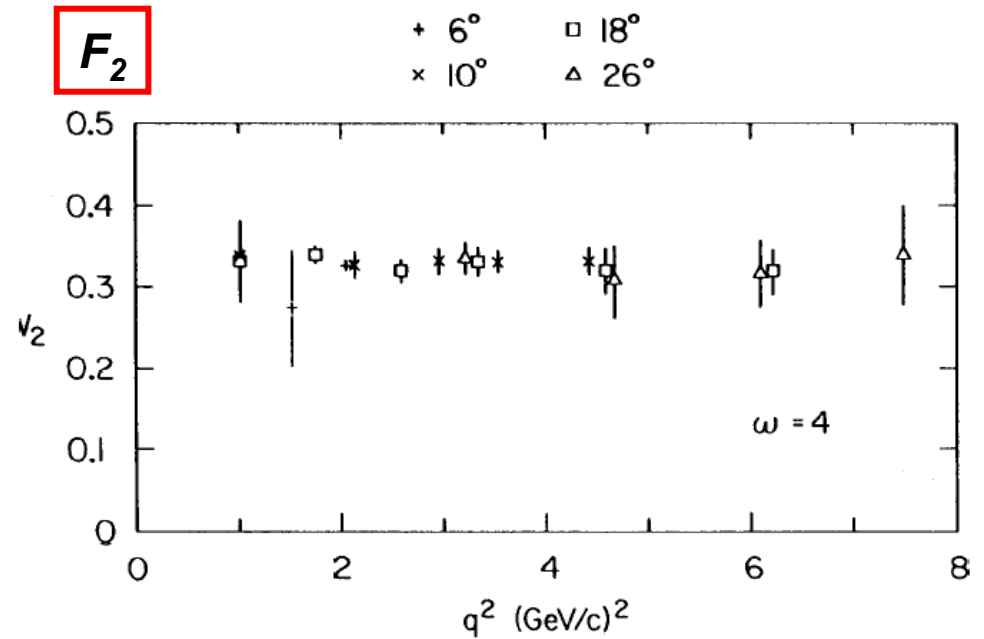
First SLAC-MIT results

Two unexpected results...

Deep-inelastic scattering (DIS)



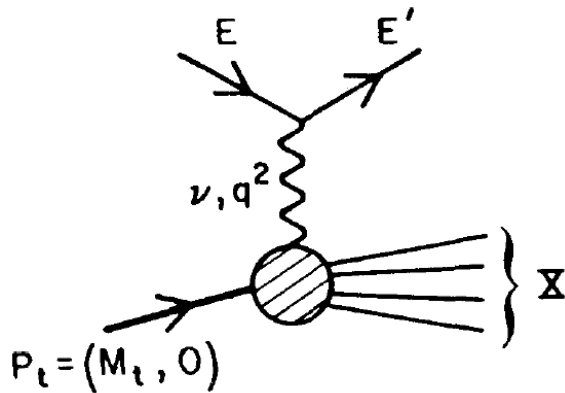
Scaling behavior



$$\omega = 1/x$$

Deep inelastic scattering (DIS) and structure Fs

Kinematic variables



$$\nu = \frac{P \cdot q}{\sqrt{P \cdot P}} = E_1 - E_2$$

$$x = \frac{-q^2}{2P \cdot q} = \frac{Q^2}{2M\nu}$$

$$Q^2 = 2E_1E_2(1 - \cos \theta)$$

$$\frac{d^2\sigma}{d\Omega dE'}(E, E', \theta) = \sigma_M [W_2(\nu, q^2) + 2W_1(\nu, q^2)\tan^2(\theta/2)]$$

$$2MW_1(\nu, q^2) = F_1(\omega)$$

$$\nu W_2(\nu, q^2) = F_2(\omega)$$

Bjorken scaling (1969)
(Predicted prior to data)

$$\omega = 1/x$$

Quantum Chromodynamics

Fields: Quarks $\psi_{\text{flavor}}^{\text{color}}$ and Gluon $G^{\text{color}}(A \cdot T, g)$.

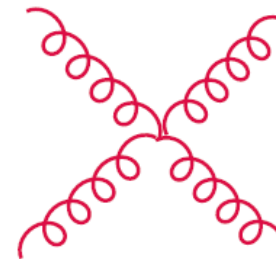
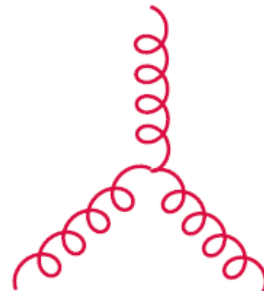
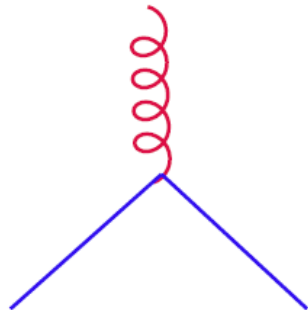
Basic Lagrangian:

$$\mathcal{L} = \bar{\psi}(i \not{\partial} - g \not{A} \cdot t - m)\psi - \frac{1}{4}G(A \cdot T, g) \cdot G(A \cdot T, g)$$

- g : gauge Coupling Strength
- m_i : quark masses
- t & T : color SU(3) matrices in the fundamental and adjoint representations.

Group factors: $C_F = \frac{4}{3}$; $T_F = \frac{1}{2}$; $C_A = 3$

Interaction Vertices:



Why does QCD play such a crucial role in High Energy Phenomenology?

- The parton picture language provides the foundation on which all modern particle theories are formulated, and all experimental results are interpreted.
- The validity of the parton picture is based empirically on an overwhelming amount of experimental evidence collected in the last 30-40 years, and theoretically on the Factorization Theorems of PQCD.

How could the *simple* (almost non-interacting) *parton picture* possibly hold in QCD — a strongly interacting quantum gauge field theory?

Answer: 3 unique features of QCD:

1. **Asymptotic Freedom:**

A strongly interacting theory at long-distance can become weakly interacting at short-distance.

2. **Infra-red Safety:**

There are classes of infra-red safe quantities which are independent of long-distance physics, hence are calculable in PQCD.

3. **Factorization:**

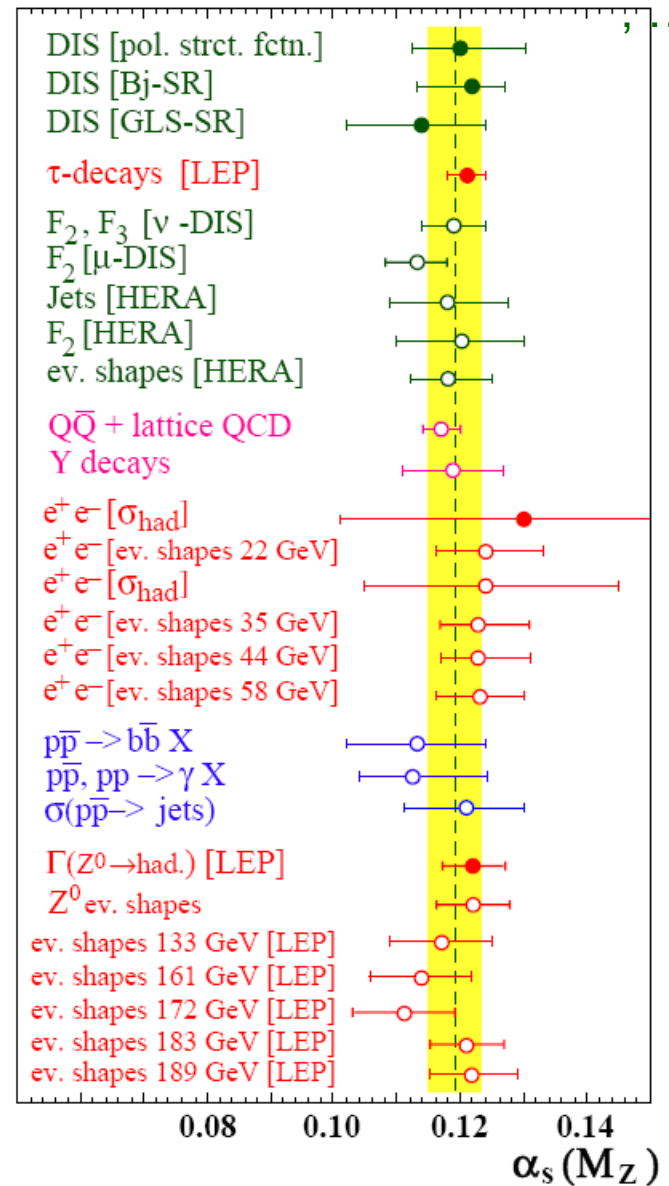
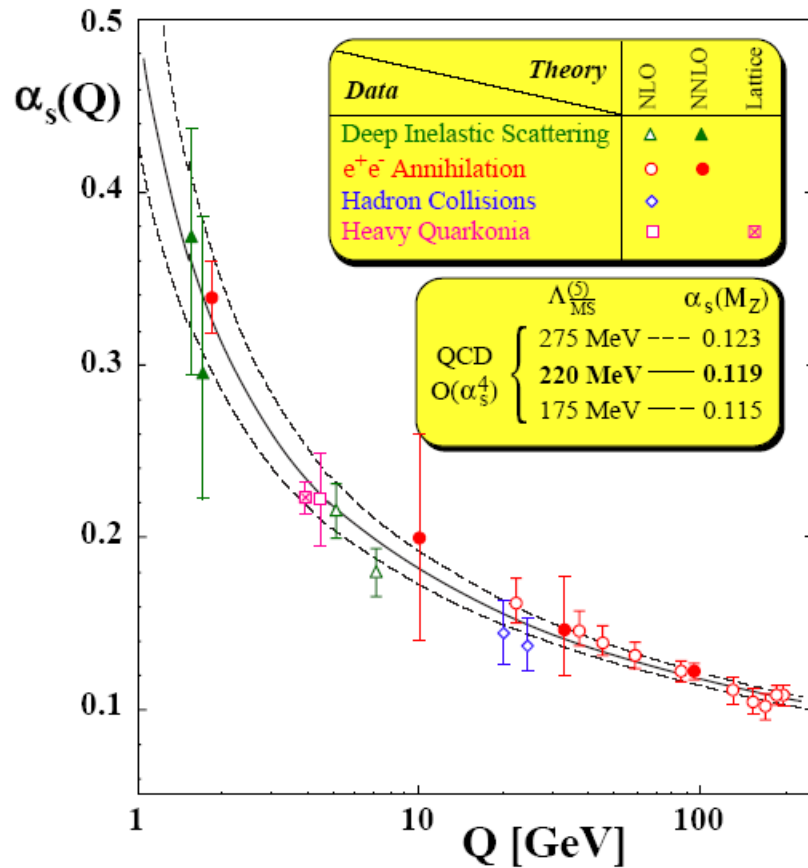
There are an even wider class of physical quantities which can be factorized into a long-distance piece (not calculable, but *universal*) and short-distance piece (process-dependent, but infra-red safe, hence *calculable*).

Key concepts: Ultra-violet divergences, bare Green fns, renormalization, RGE, anomalous dimensions, renormalized G.Fs ... etc.

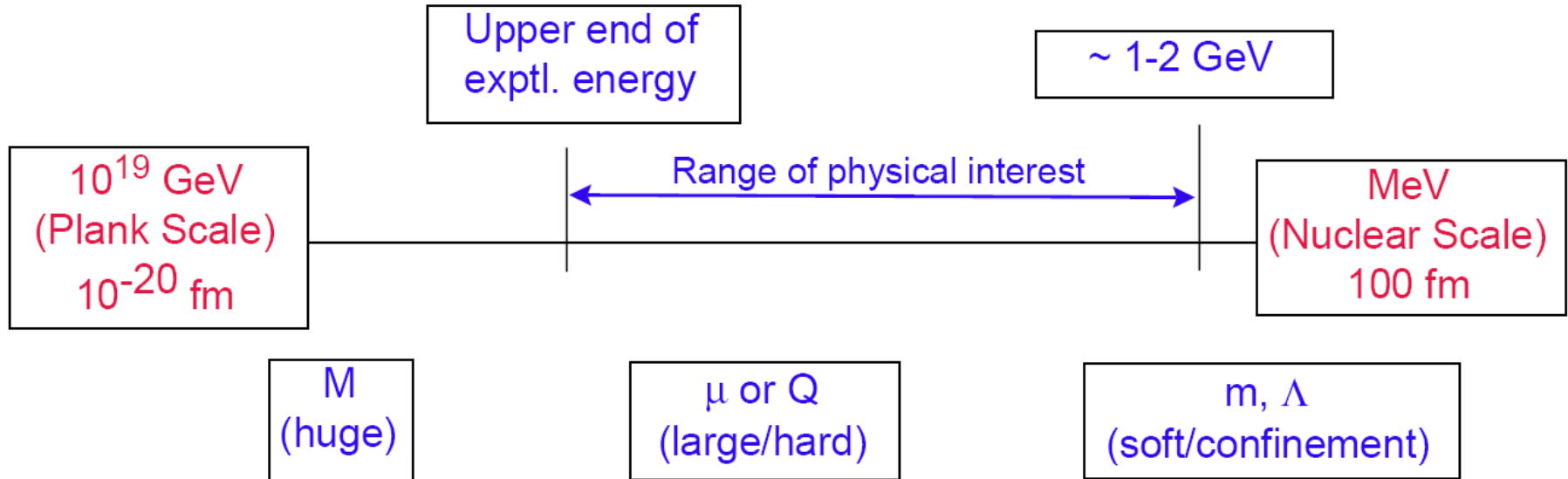
Asymptotic Freedom

Universal (running) coupling:

$$\alpha_s(Q) = \frac{g^2}{4\pi} = \frac{b}{\ln(Q/\Lambda)} (1 + \dots)$$



The importance of *Scales* -- Renormalization and Factorization



What to do with the long-distance physics associated with colinear/soft singularities in PQCD?

1st strategy:

Identify physical observables which are insensitive to the singularities! (Infra-red-safe (IRS) quantities)

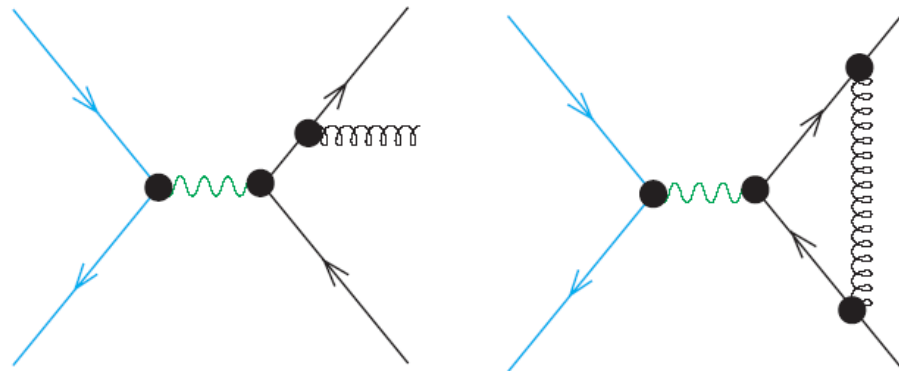
Total Hadronic Cross-section (*inclusive*):

$$\sigma_{tot}(s) = \sigma_0(s) [1 + \alpha_s(s) c_1 + \dots]$$

Block – Nordsieck Thm $\rightarrow c_{1,2,\dots}$ are finite, i.e. IRS
(unitarity)

Order α_s :

Cancellation of the colinear/soft singularities between real and virtual diagrams



Infra-Red-Safe observables:

Total hadronic Cross-section $\sigma_{\text{tot}}/\sigma_{\mu+\mu^-}$

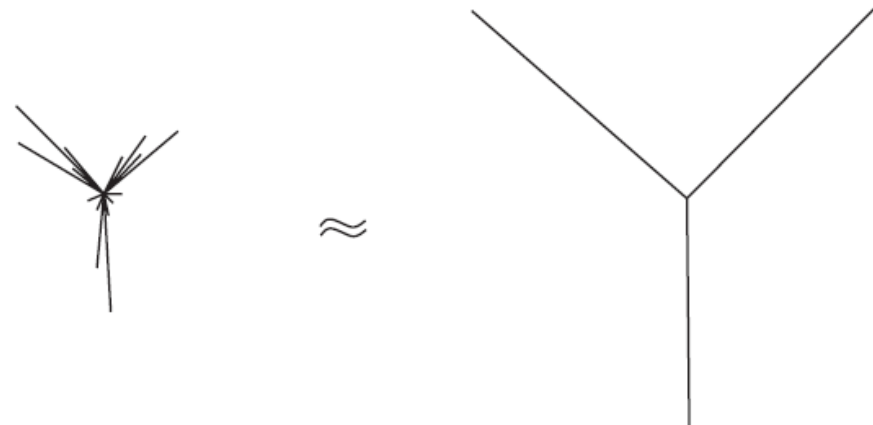
Sterman-Weinberg jet cross-sections and their modern variations (*Jade-, Durham-, ... algorithms*);

Jet shape observables: Thrust, ... ;

energy-energy correlation ;

Essential feature of a general IRS physical quantity:

the observable must be such that it is insensitive to whether n or $n+1$ particles contributed -- if the $n+1$ particles has n -particle kinematics



e.g. a IRS "jet algorithm"

σ and R in e^+e^- Collisions

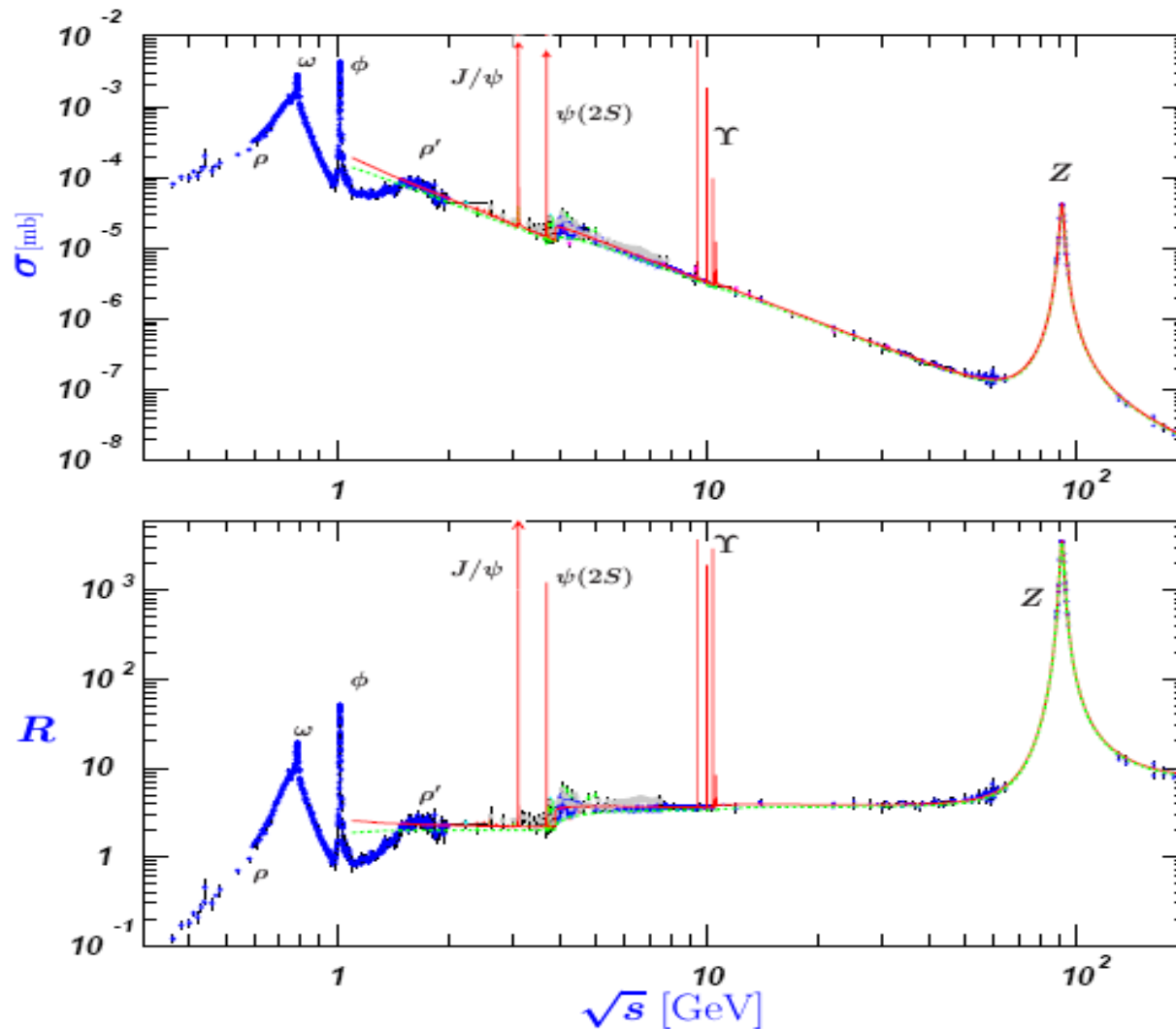
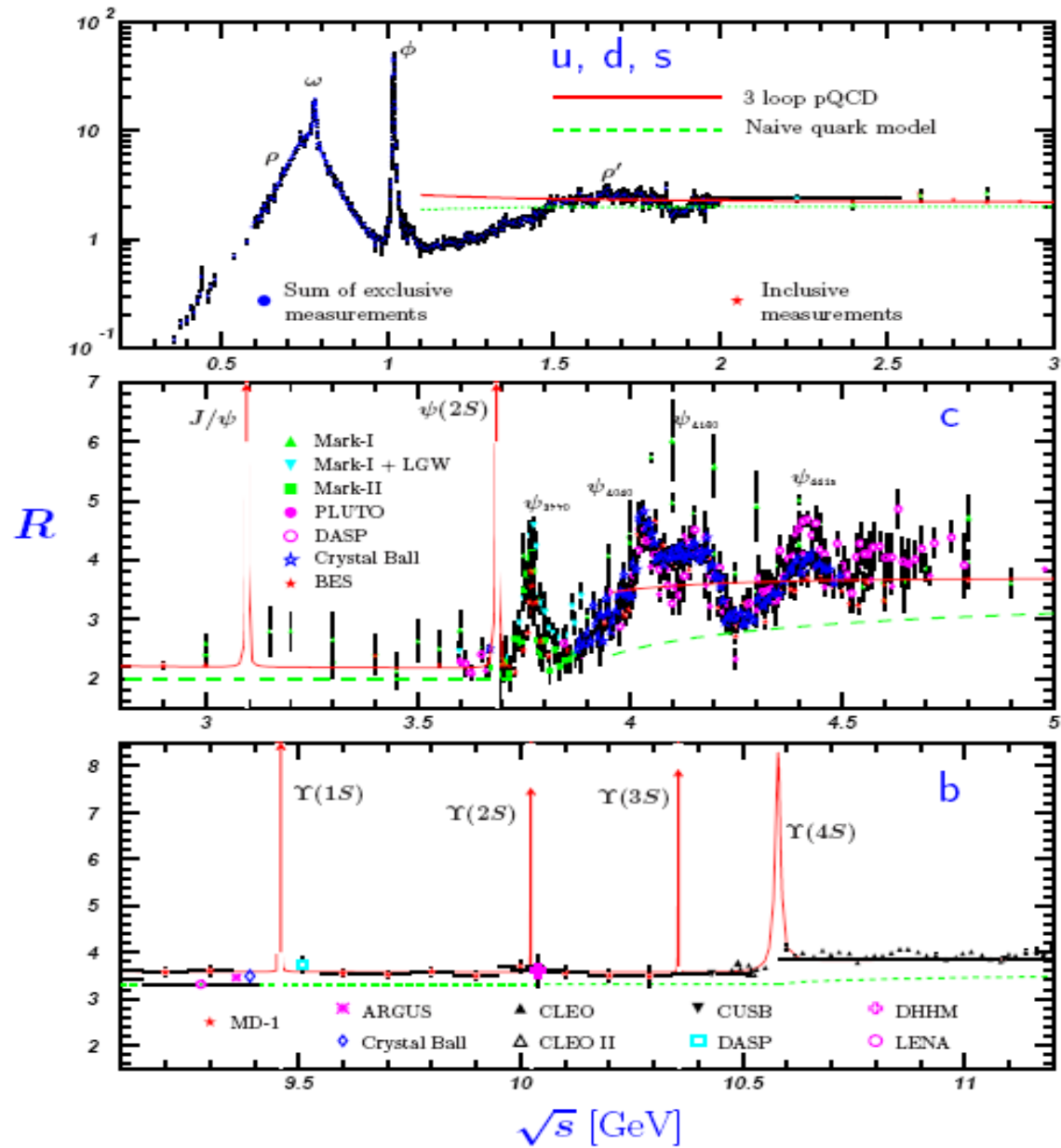


Figure 40.6: World data on the total cross section of $e^+e^- \rightarrow \text{hadrons}$ and the ratio $R(s) = \sigma(e^+e^- \rightarrow \text{hadrons}, s) / \sigma(e^+e^- \rightarrow \mu^+\mu^-, s)$. $\sigma(e^+e^- \rightarrow \text{hadrons}, s)$ is the experimental cross section corrected for initial state radiation and electron-positron vertex loops, $\sigma(e^+e^- \rightarrow \mu^+\mu^-, s) = 4\pi\alpha^2(s)/3s$. Data errors are total below 2 GeV and statistical above 2 GeV. The curves are an educative guide: the broken one (green) is a naive quark-parton model prediction and the solid one (red) is 3-loop pQCD prediction (see “Quantum Chromodynamics” section of this Review, Eq. (9.12) or, for more details, K. G. Chetyrkin *et al.*, Nucl. Phys. B586, 56 (2000) (Erratum *ibid.* B634, 413 (2002)). Breit-Wigner parameterizations of J/ψ , $\psi(2S)$, and $\Upsilon(nS)$, $n = 1, 2, 3, 4$ are also shown. The full list of references to the original data and the details of the R ratio extraction from them can be found in [arXiv:hep-ph/0312114]. Corresponding computer-readable data files are available at <http://pdg.ihep.su/xsect/contents.html>. (Courtesy of the COMPAS(Protvino) and HEPDATA(Durham) Groups, August 2005. Corrections by P. Janot (CERN) and M. Schmitt (Northwestern U.)) See full-color version on color pages at end of book.

R in Light-Flavor, Charm, and Beauty Threshold Regions



The 2nd strategy:

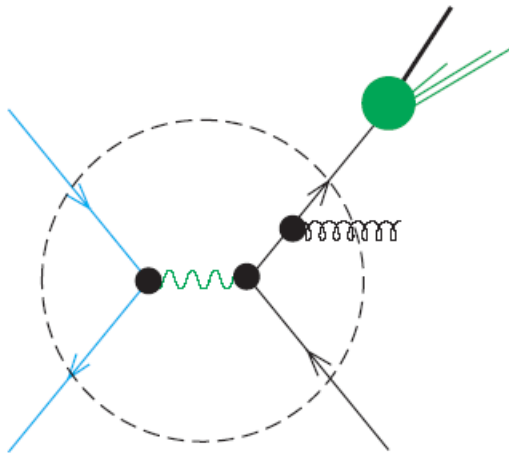
Factorization



QCD Parton model

Factorize the physical observable into a calculable *IRS* part and a non-calculable but *universal* piece.

Example: One particle inclusive cross-section



Fragmentation function:
Long-distance physics;
Universal.

Hard scattering:
Short distance physics;
IRS, perturbatively cal.

$$\sigma(s, z) = \int_z^1 \frac{d\zeta}{\zeta} \hat{\sigma}^a \left(\frac{s}{\mu}, \frac{z}{\zeta}, \alpha_s(\mu) \right) \cdot D_a(\zeta, \mu)$$

“Renormalization” and “Factorization”

UV renormalization		Collinear/soft factorization	
A: Bare Green Func.	$G_0(\alpha_0, m_0, ..)$	Partonic X-sect	F_a
B: Ren. constants	$Z_i(\mu)$	Pert. parton dist.	$f_a^b(\mu)$
C: Ren. Green Fun.	$G_R = G_0/Z$	Hard X-sect	$\hat{F} = F / f$
D: Anomalous dim.	$\gamma = \frac{\mu}{Z} \frac{d}{d\mu} Z$	Splitting fun.	$P = \frac{\mu}{f} \frac{d}{d\mu} f$
E: Phys. para. α, m	$\alpha_0 Z_i \dots$	Had. parton dist. f_A	resummed
F: Phys sc. amp.	$\alpha(\mu) G_R(m, \mu)$	Hadronic S.F.'s F_A	$f_A(\mu) \times \hat{F}(\mu)$

Some common features:

A : divergent; but, independent of “scheme” and scale μ ;

B : divergent; scale and scheme dependent;
universal; absorbs all ultra-violet/soft/collinear divergences;

C & D : finite; scheme-dependent;
D controls the μ dependence of E & F;

E : physical parameters to be obtained from experiment;

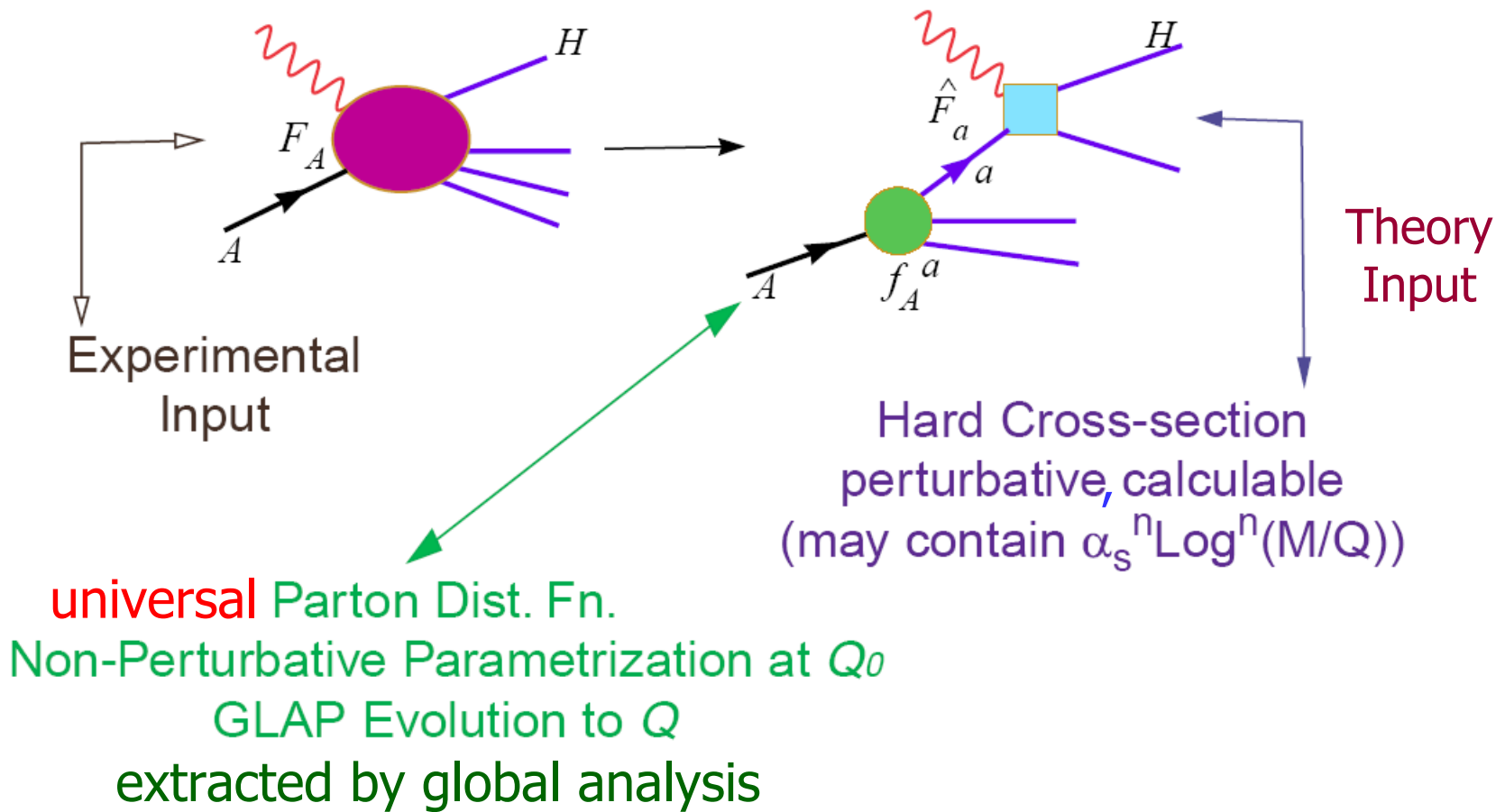
F : Theoretical “prediction”; μ -indep. to all orders,
but μ -dep. at finite order n ; $\mu \frac{d}{d\mu} \sim \mathcal{O}(\alpha^{n+1})$

Note: “Renormalization” is factorization (of UV divergences);
“factorization” is renormalization (of soft/collinear div.)

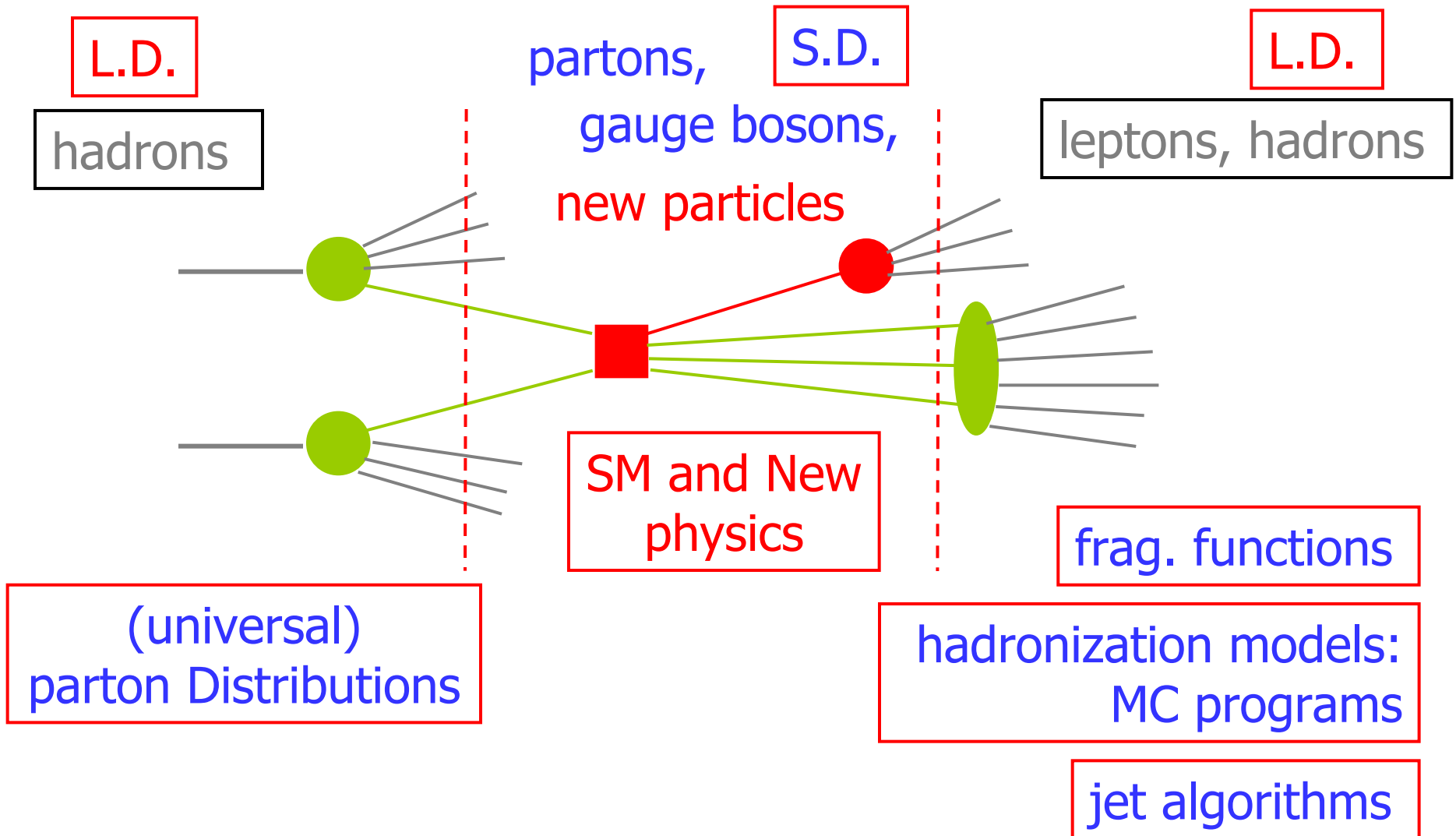
Lepton-hadron Sc.

Master Equation for QCD Parton Model
 – the Factorization Theorem

$$F_A^\lambda(x, \frac{m}{Q}, \frac{M}{Q}) = \sum_a f_A^a(x, \frac{m}{\mu}) \otimes \hat{F}_a^\lambda(x, \frac{Q}{\mu}, \frac{M}{Q}) + \mathcal{O}((\frac{\Lambda}{Q})^2)$$



Hadron Collider Physics



Deep Inelastic Scattering (DIS) in Lepton-Hadron Collisions

Probing the Parton Structure of the
Nucleon with Leptons

Deep Inelastic Scattering in Lepton-Hadron Collisions

— Probing the Parton Structure of the Nucleon with Leptons

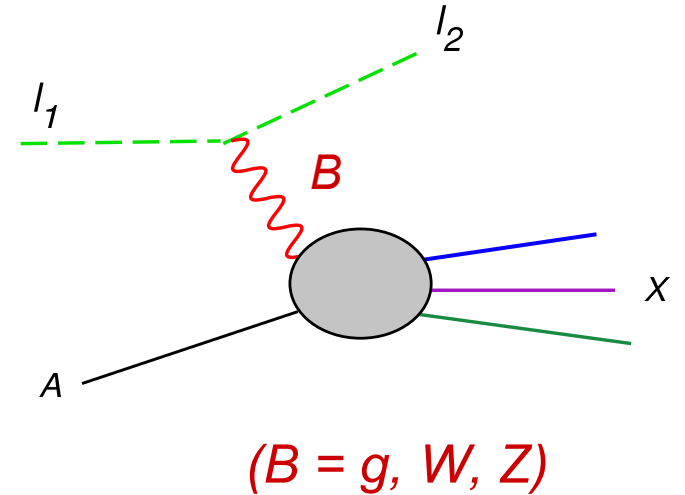
- **Basic Formalism**
(indep. of strong dynamics and parton picture)
- **Experimental Development**
 - Fixed target experiments
 - HERA experiments
- **Parton Model and QCD**
 - Parton Picture of Feynman-Bjorken
 - Asymptotic freedom, factorization and QCD
- **Phenomenology**
 - QCD parameters
 - Parton distribution functions
 - Other interesting topics

Basic Formalism

(leading order in EW coupling)

Lepton-hadron scattering process

$$l_1(l_1) + N(P) \longrightarrow l_2(l_2) + X(P_X)$$



Effective fermion-boson electro-weak interaction Lagrangian:

$$\mathcal{L}_{\text{int}}^{\text{EW}} = -g_B \left[j_{\mu}^{(\ell)}(x) + J_{\mu}^{(h)}(x) \right] V_B^{\mu}(x)$$

EW SU(2)xU(1) gauge coupling constants

B	γ	W^{\pm}	Z
g_B	$-e$	$\frac{g}{2\sqrt{2}}$	$\frac{g}{2 \cos \theta_W}$

Basic Formalism: Scattering Amplitudes

Scattering Amplitudes

$$\mathcal{M} = J_{\mu}^{*}(P, q) \frac{g_B^2 G^{\mu}_{\nu}}{Q^2 + M_B^2} j^{\nu}(q, \ell)$$

Spin 1 projection tensor

$$G^{\mu}_{\nu} = g^{\mu}_{\nu} - q^{\mu} q_{\nu} / M_B^2.$$

Lepton current amplitude (known):

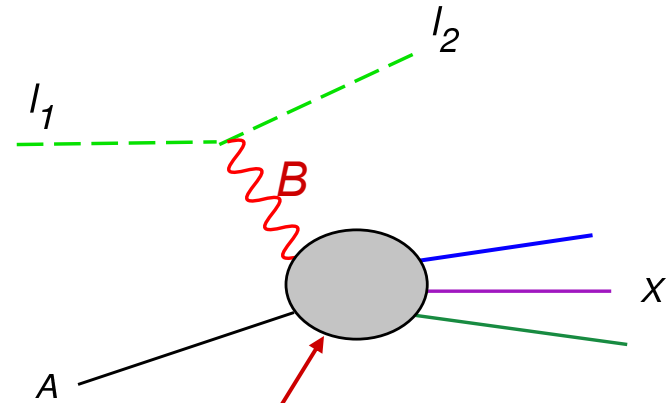
$$j^{\mu}(q, \ell) = \langle \ell_2 | j^{\mu} | \ell_1 \rangle = \bar{u}(\ell_2) \gamma^{\mu} [g_R(1 + \gamma^5) + g_L(1 - \gamma^5)] u(\ell_1)$$

Hadron current amplitude (unknown):

$$J_{\mu}^{*}(P, q) = \langle P_X | J_{\mu}^{\dagger} | P \rangle$$

Object of study:

- * Parton structure of the nucleon; (short distance)
- * QCD dynamics at the confinement scale (long dis.)



Basic Formalism: Cross section

Cross section

(amplitude)² phase space / flux

$$d\sigma = \frac{G_1 G_2}{2\Delta(s, m_{\ell_1}^2, M^2)} 4\pi Q^2 L_\nu^\mu W_\mu^\nu d\Gamma$$

$$G_i = g_{B_i}^2 / (Q^2 + M_{B_i}^2)$$

Lepton tensor (known):

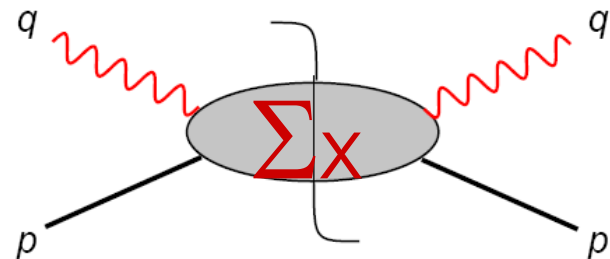
$$L_\nu^\mu = \frac{1}{Q^2} \overline{\sum_{\text{spin}}} \langle \ell_1 | j_\nu^\dagger | \ell_2 \rangle \langle \ell_2 | j^\mu | \ell_1 \rangle$$

Hadron tensor (unknown):

$$W_\nu^\mu = \frac{1}{4\pi} \overline{\sum_{\text{spin}}} (2\pi)^4 \delta^4(P + q - P_X) \langle P | J^\mu | P_X \rangle \langle P_X | J_\nu^\dagger | P \rangle$$

Object of study:

- * Parton structure of the nucleon;
- * QCD dynamics at the confinement scale



Basic Formalism: Structure Functions

Expansion of W^μ_ν in terms of independent components

$$W^\mu_\nu = -g^\mu_\nu W_1 + \frac{P^\mu P_\nu}{M^2} W_2 - i \frac{\epsilon^{Pq\mu}_\nu}{2M^2} W_3 + \\ + \frac{q^\mu q_\nu}{M^2} W_4 + \frac{P^\mu q_\nu + q^\mu P_\nu}{2M^2} W_5 + \frac{P^\mu q_\nu - q^\mu P_\nu}{2M^2} W_6$$

Cross section in terms of the structure functions

$$\frac{d\sigma}{dE_2 d\cos\theta} = \frac{2E_2^2 G_1 G_2}{\pi M n_\ell} \left\{ g_{+\ell}^2 \left[2W_1 \sin^2 \frac{\theta}{2} + W_2 \cos^2 \frac{\theta}{2} \right] \pm g_{-\ell}^2 \left[\frac{E_1 + E_2}{M} W_3 \sin^2 \frac{\theta}{2} \right] \right\}$$

Charged Current (CC) processes (neutrino beams):

W-exchange (diagonal); left-handed coupling only;

Neutral Current (NC) processes (e, μ scat.)---low energy:

(fixed tgt): γ -exchange (diagonal); vector coupling only; ...

Neutral Current (NC) processes (e, μ scat.)---high energy

(hera): γ & Z exchanges: G_1^2 , $G_1 G_2$, G_2^2 terms;

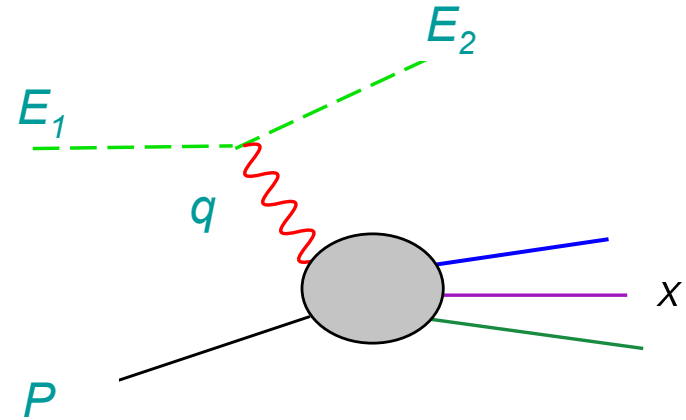
Basic Formalism: Scaling structure functions

Kinematic variables

$$\nu = \frac{P \cdot q}{\sqrt{P \cdot P}} = E_1 - E_2$$

$$x = \frac{-q^2}{2P \cdot q} = \frac{Q^2}{2M\nu}$$

$$y = \frac{P \cdot q}{P \cdot \ell_1} = \frac{\nu}{E_1}$$



Scaling (dimensionless)
structure functions

$$\begin{aligned} F_1(x, Q) &= W_1 \\ F_2(x, Q) &= \frac{\nu}{M} W_2 \\ F_3(x, Q) &= \frac{\nu}{M} W_3 \end{aligned}$$

Scaling form of cross section
formula:

$$\left(g_{\pm\ell}^2 = g_{L\ell}^2 \pm g_{R\ell}^2 \right)$$

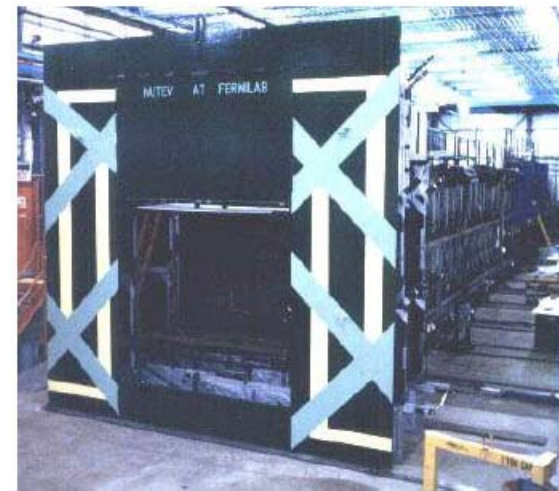
$$\frac{d\sigma}{dx dy} = \frac{2ME_1}{\pi} \frac{G_1 G_2}{n_\ell} \left\{ g_{+\ell}^2 \left[xF_1 y^2 + F_2 \left[(1-y) - \left(\frac{Mxy}{2E_1} \right) \right] \right] \pm g_{-\ell}^2 \left[xF_3 y \left(1 - \frac{y}{2} \right) \right] \right\}$$

n_ℓ is the number of polarization states of the incoming lepton.

The highest energy (anti-) neutrino DIS experiment

The NuTeV experiment at FNAL

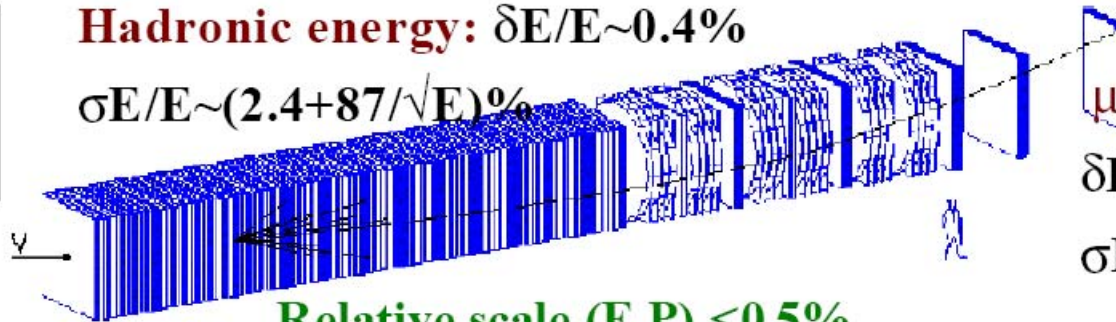
ν -N DIS, sign-selected beam $\langle E_\nu \rangle \sim 120$ GeV
and continuous test beam calibration



Data taken during 1996-97

Hadronic energy: $\delta E/E \sim 0.4\%$

$\sigma E/E \sim (2.4 + 87/\sqrt{E})\%$



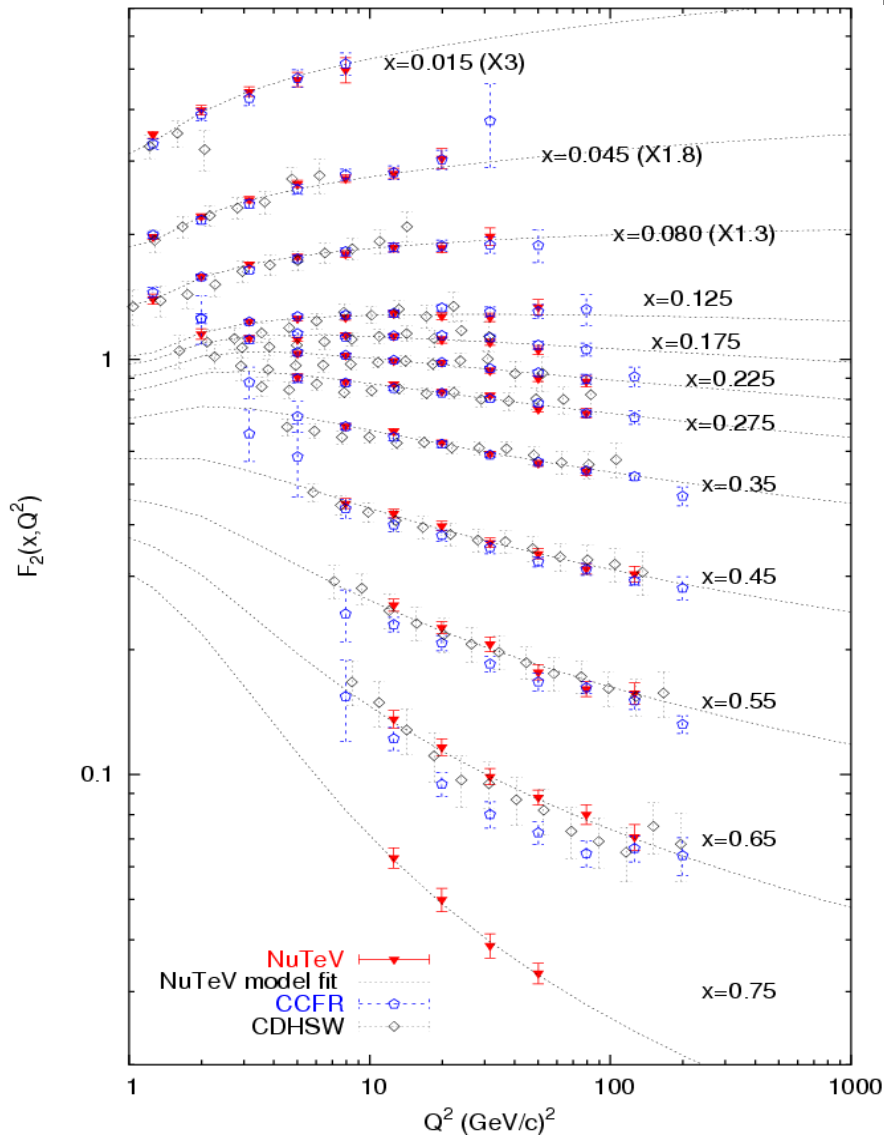
Relative scale (E,P) < 0.5%

μ momentum

$\delta P/P \sim 1\%$

$\sigma P/P \sim 11\%$

F_2 Measurement

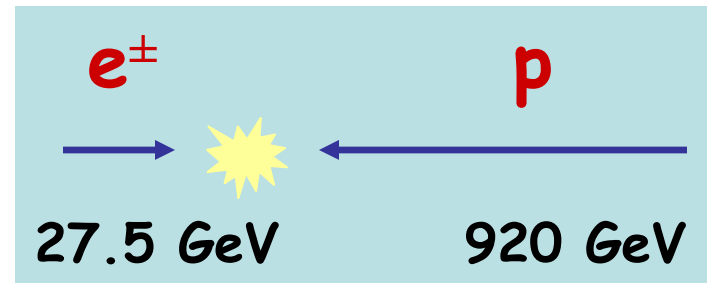


- Isoscalar ν -Fe F_2
- **NuTeV** F_2 is compared with **CCFR** and **CDHSW** results
 - the line is a fit to **NuTeV** data
- All systematic uncertainties are included
- All data sets agree for $x < 0.4$.
- At $x > 0.4$ **NuTeV** agrees with **CDHSW**
- At $x > 0.4$ **NuTeV** is systematically above **CCFR**

The HERA Collider

The first and only ep collider in the world

Located in Hamburg



$$\sqrt{s} = 318 \text{ GeV}$$

Equivalent to fixed target experiment with 50 TeV e^{\pm}

The Collider Experiments



H1 Detector

Complete 4π detector with

Tracking
Si- μ VTX
Central drift chamber

Liquid Ar calorimeter

→ $\hat{E}=E = 12\% = \sqrt{E[\text{GeV}]}$ (e:m:)

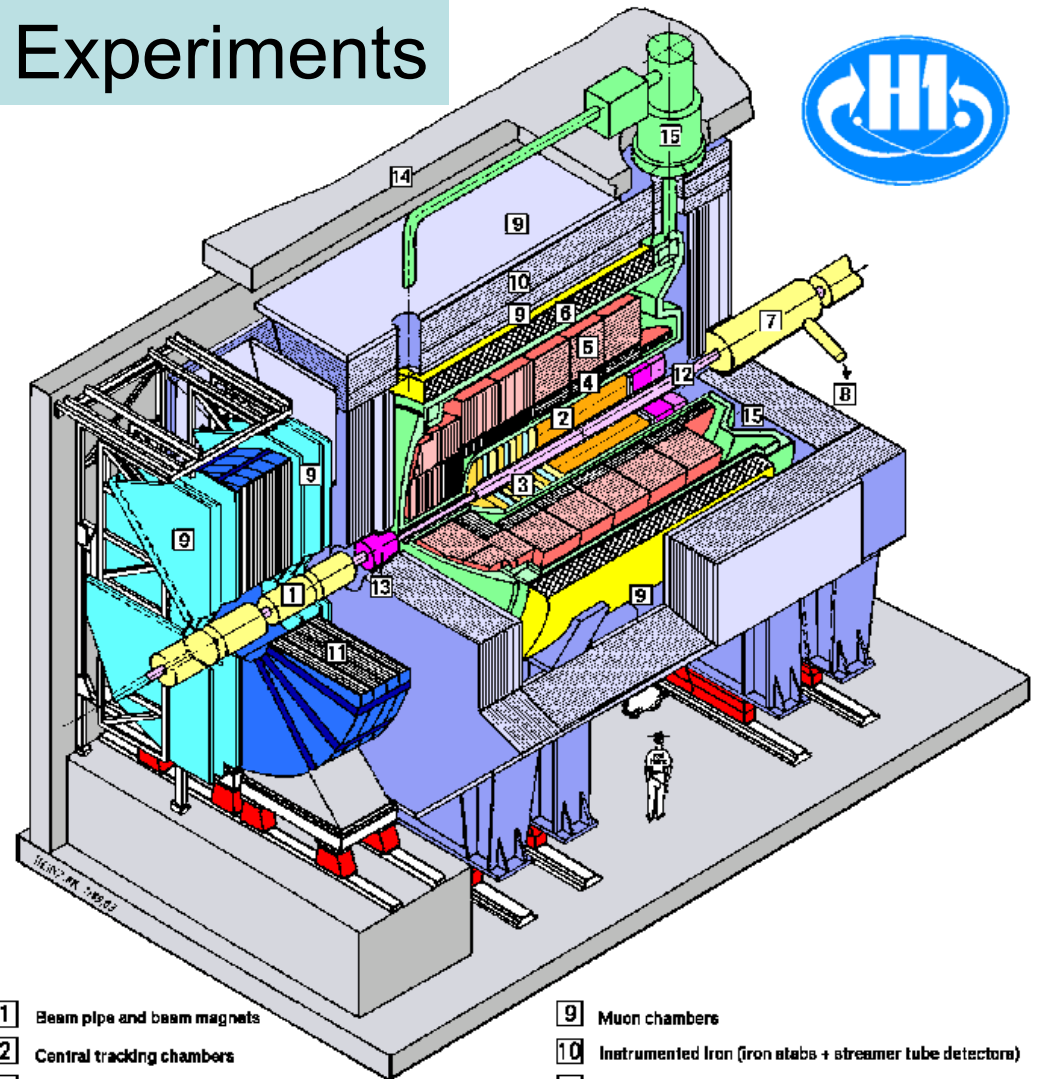
$\hat{E}=E = 50\% = \sqrt{E[\text{GeV}]}$ (had)

Rear Pb-scintillator calorimeter

→ $\hat{E}=E = 7.5\% = \sqrt{E[\text{GeV}]}$ (e:m:)

μ chambers

and much more...



- | | | | |
|---|---|----|--|
| 1 | Beam pipe and beam magnets | 9 | Muon chambers |
| 2 | Central tracking chambers | 10 | Instrumented Iron (iron slabs + streamer tube detectors) |
| 3 | Forward tracking and Transition radiators | 11 | Muon toroid magnet |
| 4 | Electromagnetic Calorimeter (lead) | 12 | Warm electromagnetic calorimeter |
| 5 | Hadronic Calorimeter (stainless steel) | 13 | Plug calorimeter (Cu, Si) |
| 6 | Superconducting coil (1.2T) | 14 | Concrete shielding |
| 7 | Compensating magnet | 15 | Liquid Argon cryostat |
| 8 | Helium cryogenics | | |
- } Liquid Argon

ZEUS Detector



Complete 4π detector with

Tracking
Si- μ VTX
Central drift chamber

Uranium-Scintillator calorimeter

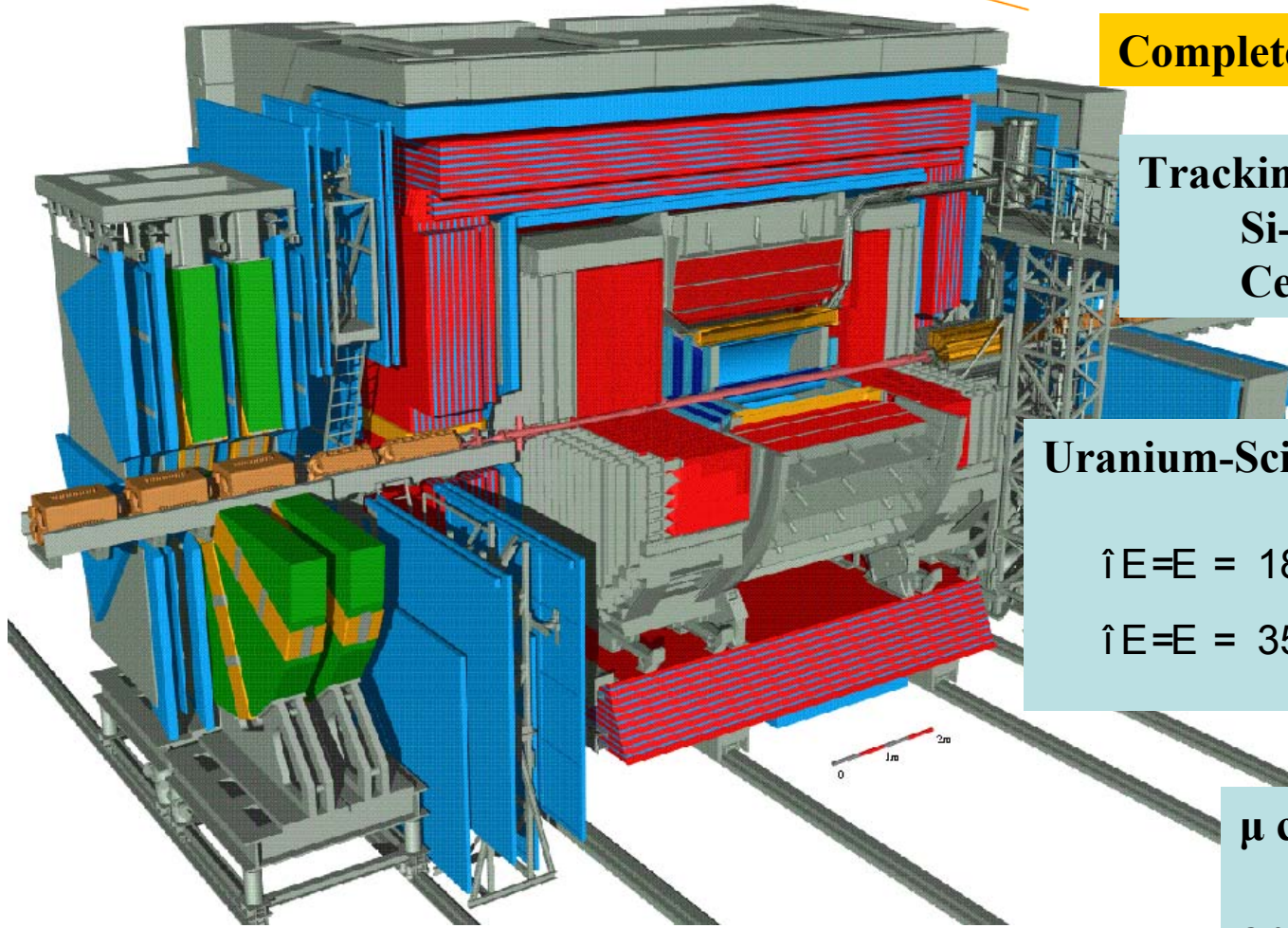
$$\hat{E} = E = 18\% = \sqrt{E[\text{GeV}]} (\text{e.m.})$$

$$\hat{E} = E = 35\% = \sqrt{E[\text{GeV}]} (\text{had})$$

μ chambers

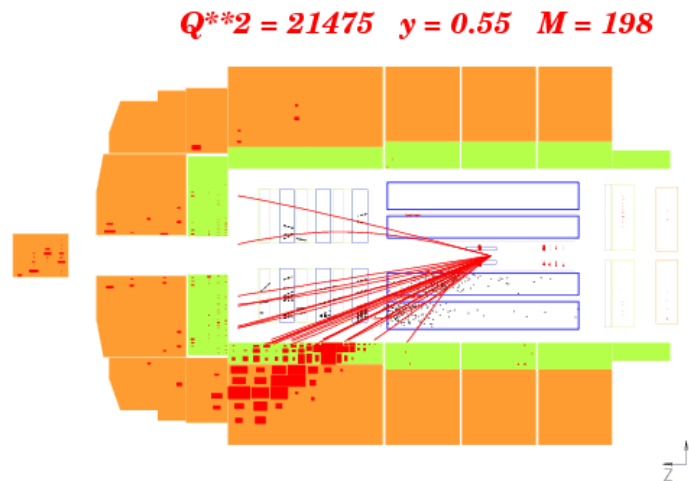
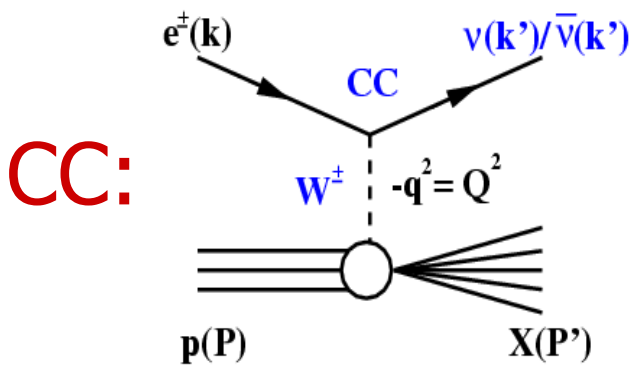
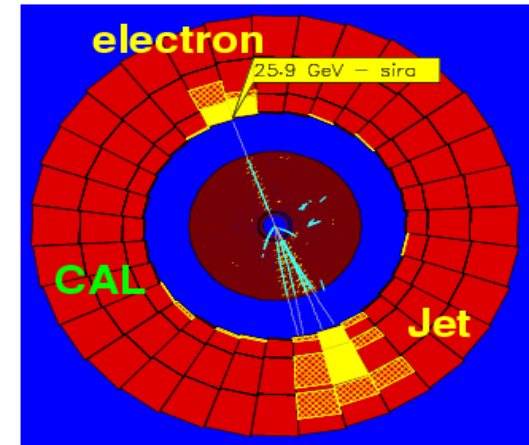
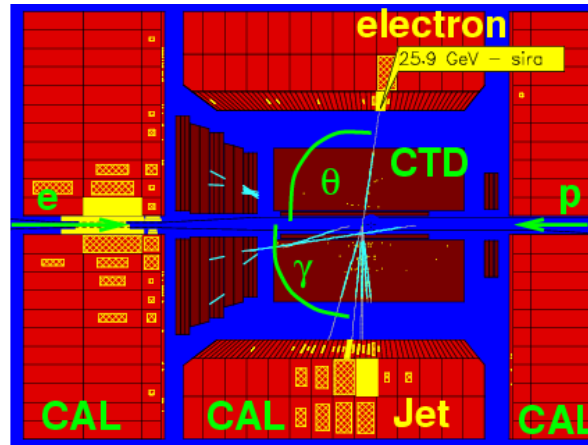
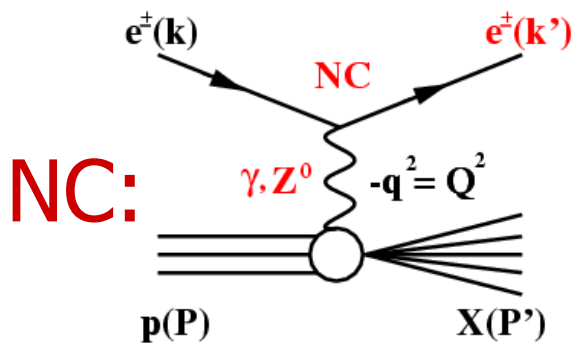
and much more...

Both detectors asymmetric



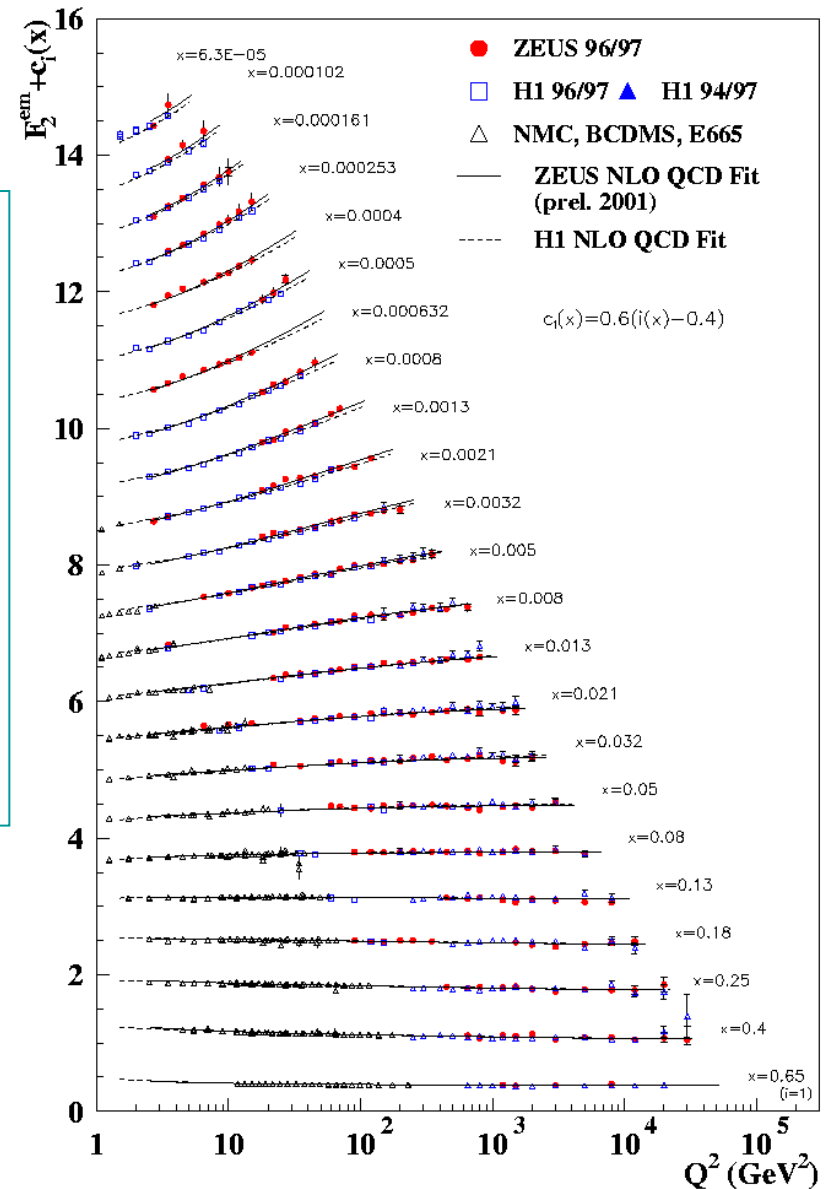
NC and CC incl. Processes measured at HERA

NC: $e^\pm + p \rightarrow e^\pm + X$, CC: $e^\pm + p \rightarrow \bar{\nu}_e(\nu_e) + X$



Measurement of $F_2^\gamma(x, Q^2)$

- For $Q^2 \ll M_Z^2 \rightarrow xF_3$ negligible;
- F_L only important at high y ;
- Both F_L and $xF_3 \sim$ calculable in QCD
- Correct for higher order QED radiation
- Extract $F_2(x, Q^2)$ from measurement of $\frac{d^2\hat{\sigma}^{ep}}{dx dQ^2}$

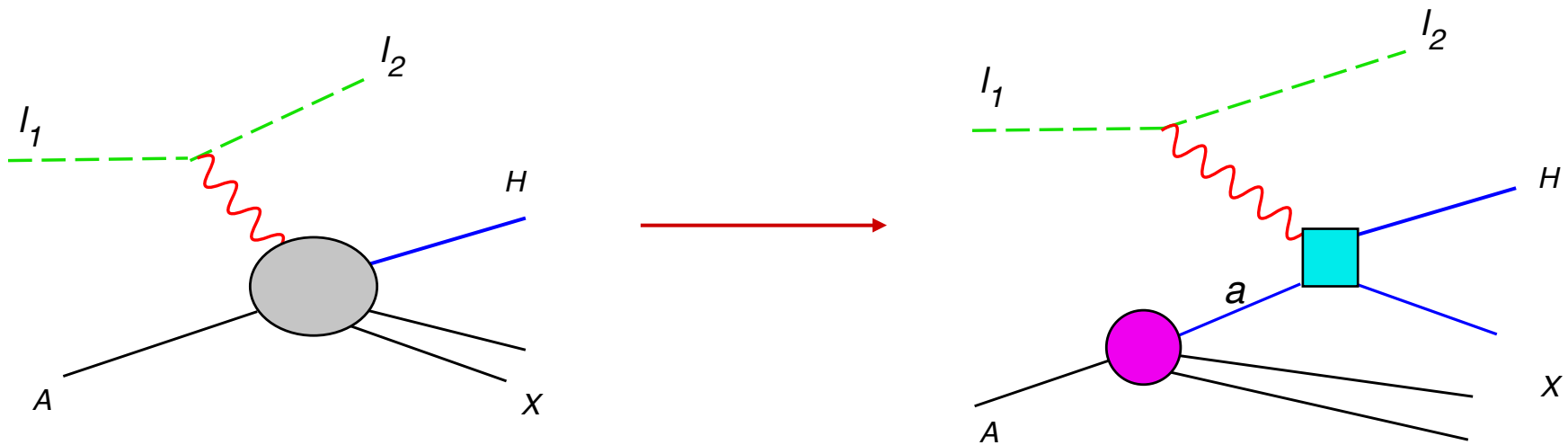


These are difficult measurements:
 nevertheless precision level has reached: errors of 2-3%

Physical Interpretations of DIS Structure Function measurements

- The Parton Model (Feynman-Bjorken)
- Theoretical basis of the parton picture and the QCD improved parton model

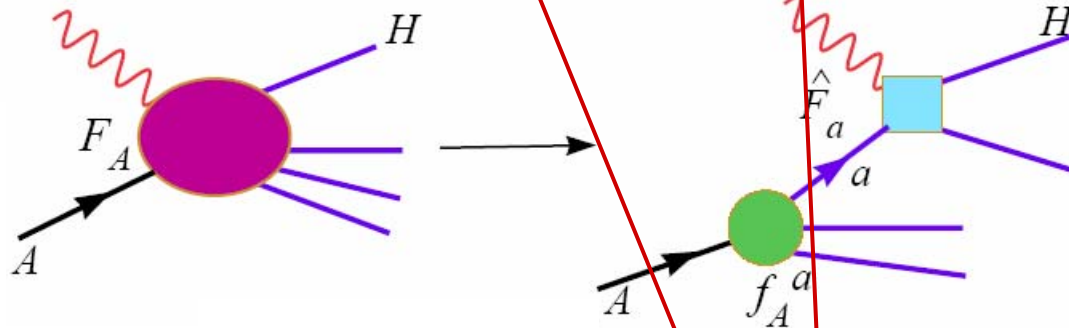
High energy (Bjorken) limit:
(large Q^2 and ν , for a fixed x value)



QCD and DIS

Master Equation for QCD Parton Model
– the Factorization Theorem

$$F_A^\lambda(x, \frac{m}{Q}, \frac{M}{Q}) = \sum_a f_A^a(x, \frac{m}{\mu}) \otimes \hat{F}_a^\lambda(x, \frac{Q}{\mu}, \frac{M}{Q}) + \mathcal{O}((\frac{\Lambda}{Q})^2)$$



A physical observable is independent of μ ,
i.e., renormalization group
invariant.

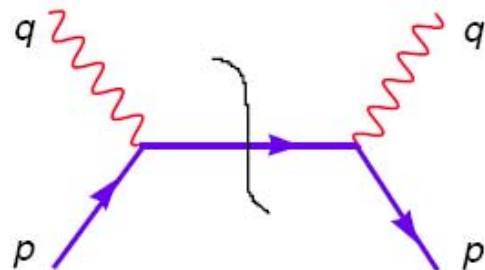
μ is the factorization scale.
Usually choose $\mu = Q$: that is
how $f(x, Q)$ acquires Q -dep.

Parton Model results on Structure Functions

$$F_{\lambda}(x, Q^2) \sim \int_0^1 \frac{d\xi}{\xi} \sum_a f_A^a(\xi) \hat{F}_{\lambda}^a(x/\xi, Q^2) + \mathcal{O}\left(\frac{m}{Q}\right).$$

where $\hat{F}_{\lambda}^a(z, Q^2)$ is the “partonic structure function” for DIS on the parton target a .

The Feynman diagram contributing to this elementary quantity and the result of a straightforward calculation are (for electro-magnetic coupling case):



$$\begin{aligned} \hat{F}_T^a(x/\xi, Q^2) &= Q_a^2 \delta(x/\xi \leftrightarrow 1) \\ \hat{F}_L^a(x/\xi, Q^2) &= 0 \\ \hat{F}_{PV}^a(x/\xi, Q^2) &= 0 \end{aligned}$$

\implies the simple scaling parton model results:

$$\begin{aligned} F_T(x, Q^2) &= \sum_a Q_a^2 f_A^a(x) && \text{(Bj. } \Leftrightarrow \text{Feynman)} \\ F_L(x, Q^2) &= 0 && \text{(Callan } \Leftrightarrow \text{Gross)} \end{aligned}$$

Structure functions: Quark Parton Model

Quark parton model (QPM) NC SFs for proton target:

$$[F_2^\gamma, F_2^{\gamma Z}, F_2^Z] = x \sum_q [e_q^2, 2e_q v_q, v_q^2 + a_q^2] \{q + \bar{q}\}$$

$$[xF_3^{\gamma Z}, xF_3^Z] = 2x \sum_q [e_q a_q, v_q a_q] \{q - \bar{q}\} = 2x \sum_{q=u,d} [e_q a_q, v_q a_q] q_v$$

QPM CC SFs for proton targets:

$$xF_{2,W^+}^{CC} = x\{\bar{u} + \bar{c} + d + s\}, \quad xF_{3,W^+}^{CC} = x\{d + s - (\bar{u} + \bar{c})\}$$

$$xF_{2,W^-}^{CC} = x\{u + c + (\bar{d} + \bar{s})\}, \quad xF_{3,W^-}^{CC} = x\{u + c - (\bar{d} + \bar{s})\}$$

For neutron targets, invoke (flavor) isospin symmetry:

$$u \Leftrightarrow d \text{ and } \bar{u} \Leftrightarrow \bar{d}$$

continued

Consequences on CC Cross sections (parton model level):

$$\frac{d\sigma^{\nu/\bar{\nu}}}{dx dy} \propto W \cdot L \propto F_{\nu/\bar{\nu}} \left(\frac{1 \pm \cosh \psi}{2} \right)^2$$

$$\cosh \psi = \frac{2-y}{y} \quad \longrightarrow \quad \frac{1 \pm \cosh \psi}{2} \propto \begin{cases} 1 \\ 1-y \end{cases}$$

$$\longrightarrow \quad \frac{\sigma^{\bar{\nu}}}{\sigma^{\nu}} = \int dy \frac{d\sigma^{\bar{\nu}}}{dy} / \int dy \frac{d\sigma^{\nu}}{dy} \approx \frac{1}{3}$$

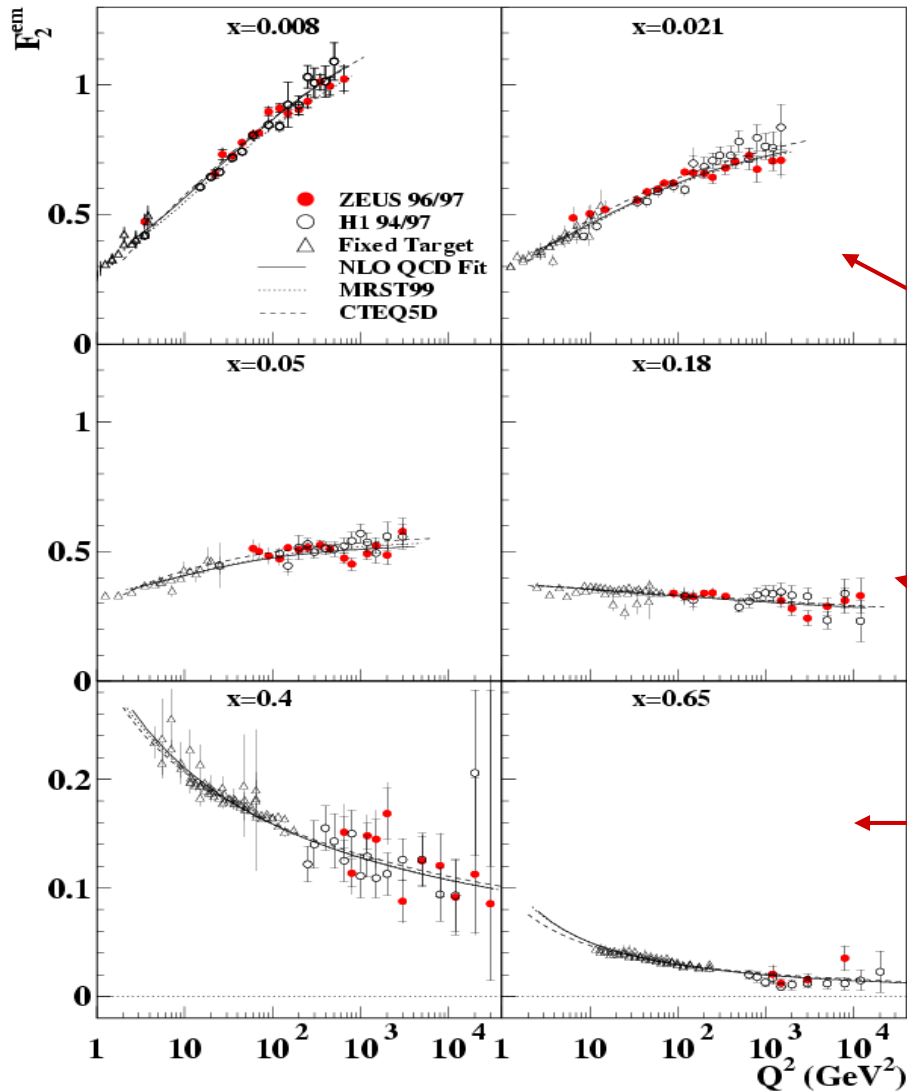
These qualitative features were verified in early (bubble chamber) high energy neutrino scattering experiments.

Gargamelle (CERN)

Refined measurements reveal QCD corrections to the approximate naïve parton model results. These are embodied in all modern “QCD fits” and “global analyses”.

F_2 : "Scaling violation" — Q -dependence inherent in QCD

ZEUS



Renormalization group equation governs the scale dependence of parton distributions and hard cross sections. (DGLAP)

Rise with increasing Q at small- x

Flat behavior at medium x

decrease with increasing Q at high x

QCD evolution

Evolution performed in terms of (1/2/3) non-singlet, singlet and gluon densities:

$$\frac{\partial}{\partial \ln \mu_F^2} q_{NS}^\pm = P_{NS}^\pm \otimes q_{NS}^\pm$$

$$\frac{\partial}{\partial \ln \mu_F^2} \begin{Bmatrix} \Sigma \\ g \end{Bmatrix} = \begin{Bmatrix} P_{qq} & P_{qg} \\ P_{gq} & P_{gg} \end{Bmatrix} \otimes \begin{Bmatrix} \Sigma \\ g \end{Bmatrix} = P \otimes q$$

Where

$$P(x) = a_s P^{(0)}(x) + a_s^2 \left[P^{(1)}(x) - \beta_0 \ln \frac{\mu_F^2}{\mu_R^2} P^{(0)}(x) \right] \quad \text{with} \quad a_s = \frac{\alpha_s(\mu_R^2)}{4\pi}$$

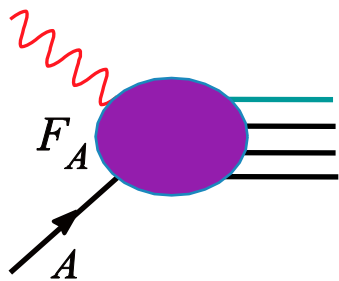
$$\frac{da_s}{d \ln \mu_R^2} = \beta(a_s) = \sum_{l=0}^{\infty} a_s^{l+2} \beta_l \cong a_s^2 \beta_0 + a_s^3 \beta_1 \quad \text{where} \quad \beta_0 = 11 - \frac{2}{3} N_F$$

$$\text{and} \quad \beta_1 = 102 - \frac{38}{3} N_F$$

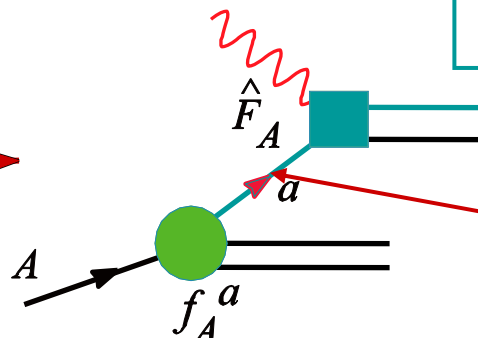
Parton Distribution Functions (PDF):
most significant physical results derived from DIS
(with help from other hard scattering processes)

A common misconception:

Parton distribution functions ~~are~~ “Structure functions”



These are the
(process-dep)
S.F.s



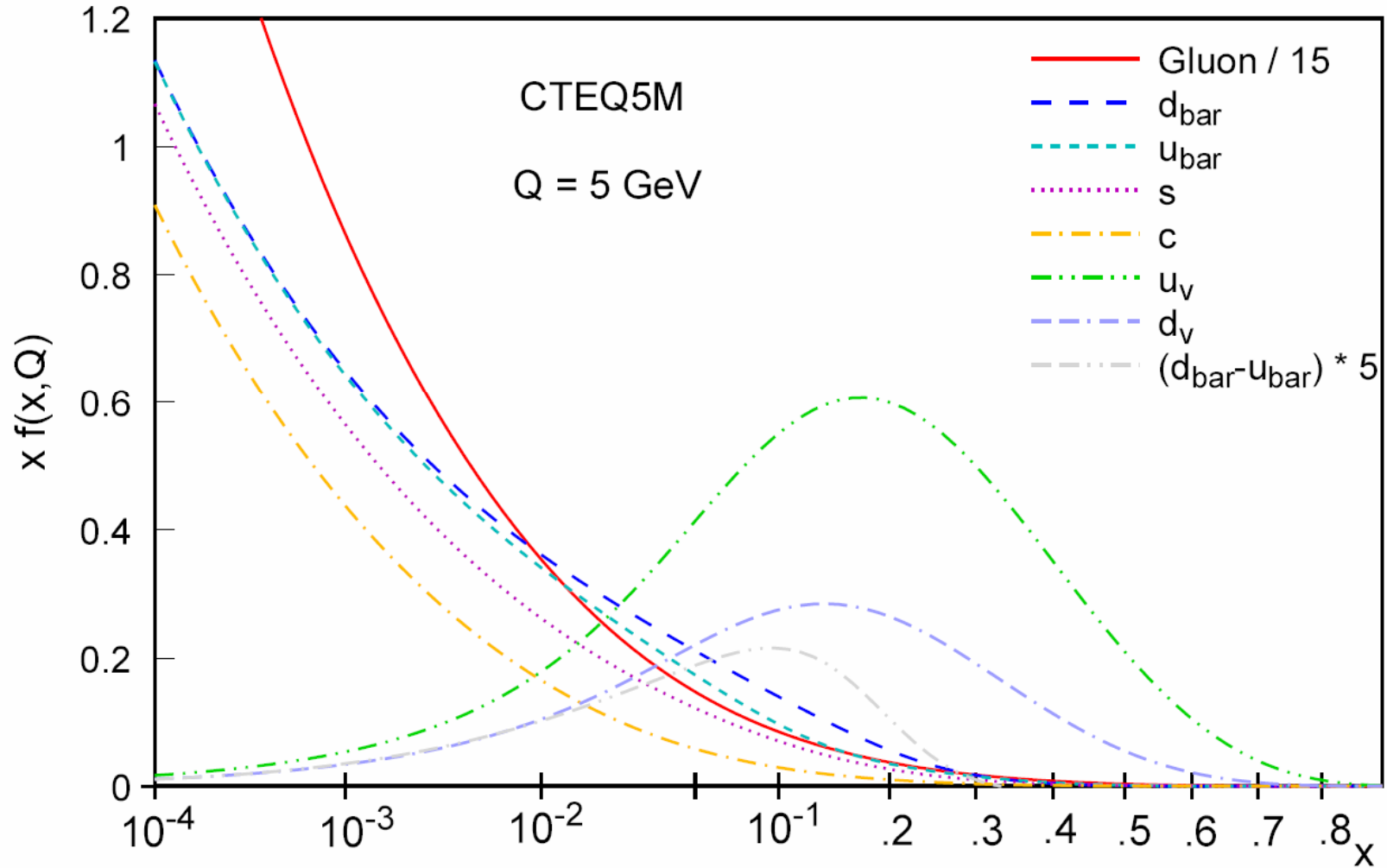
These are the
(universal)
PDFs

These are the
hard Xsecs.

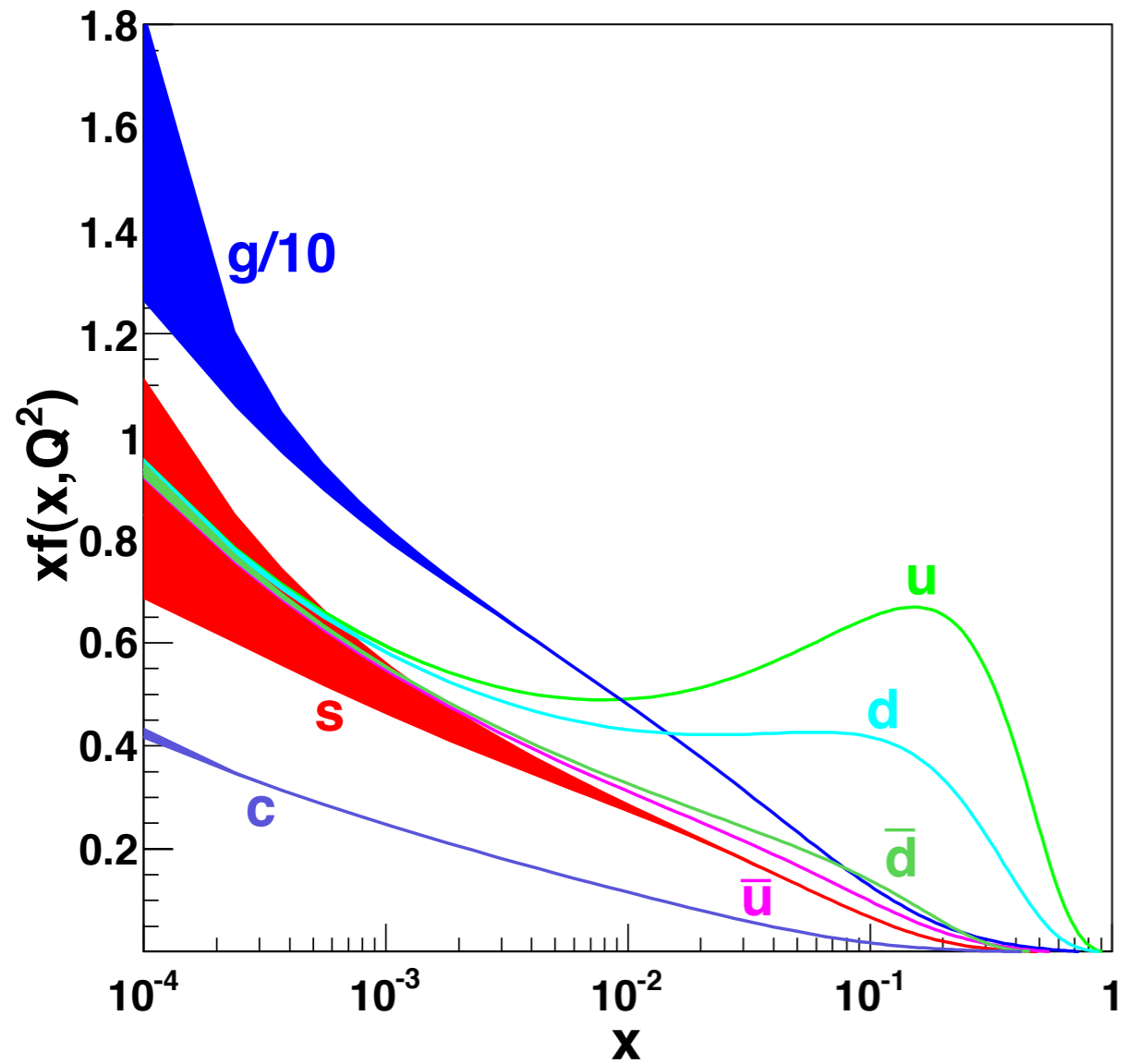
There is a convo-
lution integral and
a summation over
partons here!

Parton Distributions: one example

Overview of Parton Distribution Functions of the Proton

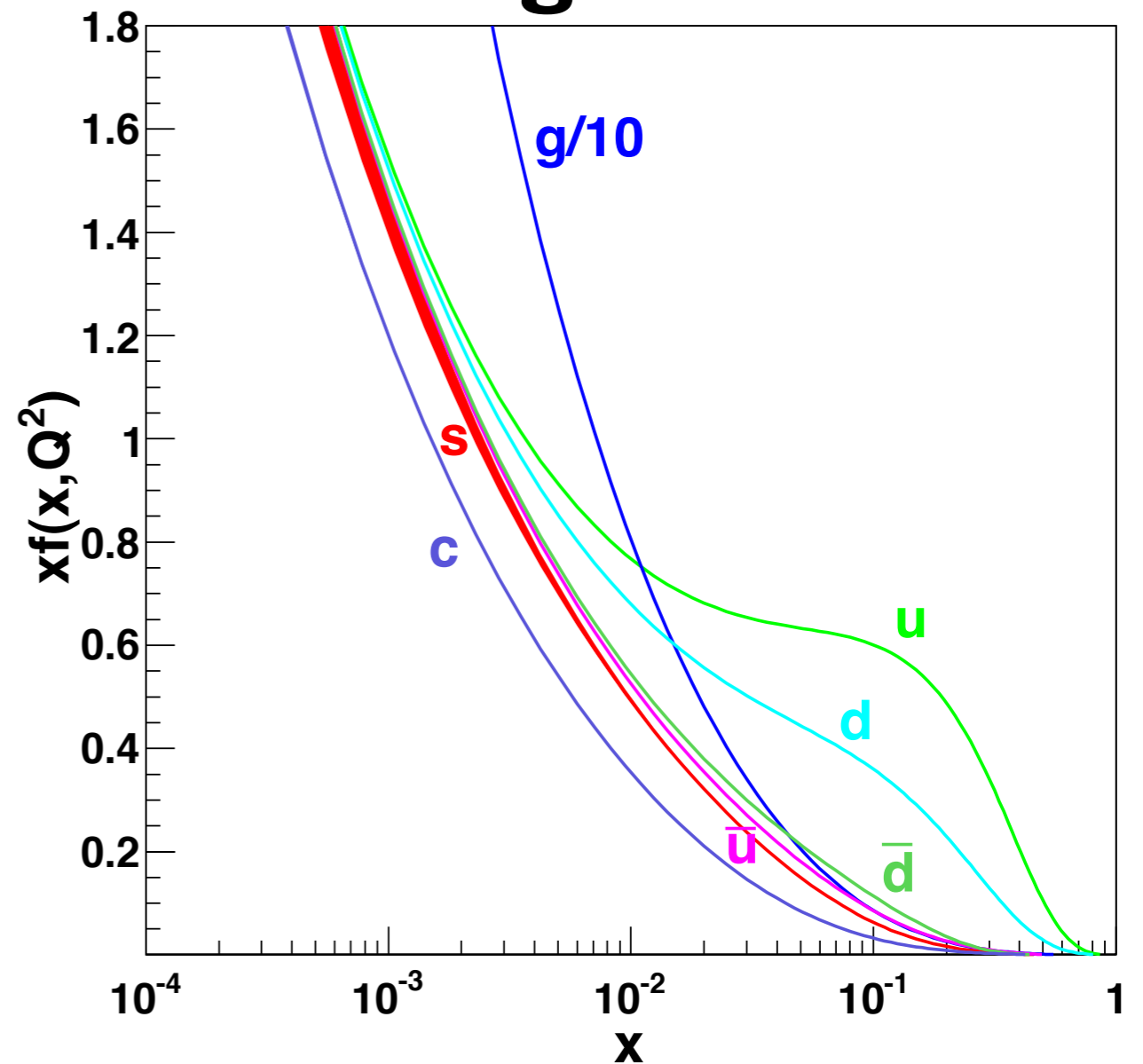


Low Scale



CT10 PDF plots

High Scale

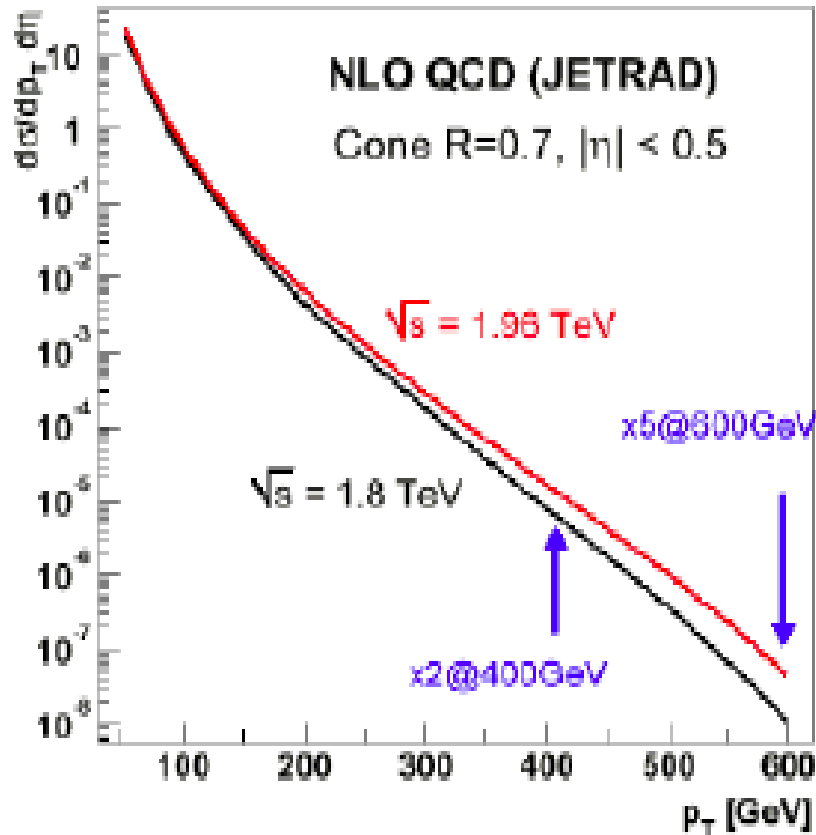


QCD in Hadron Collisions

Jets

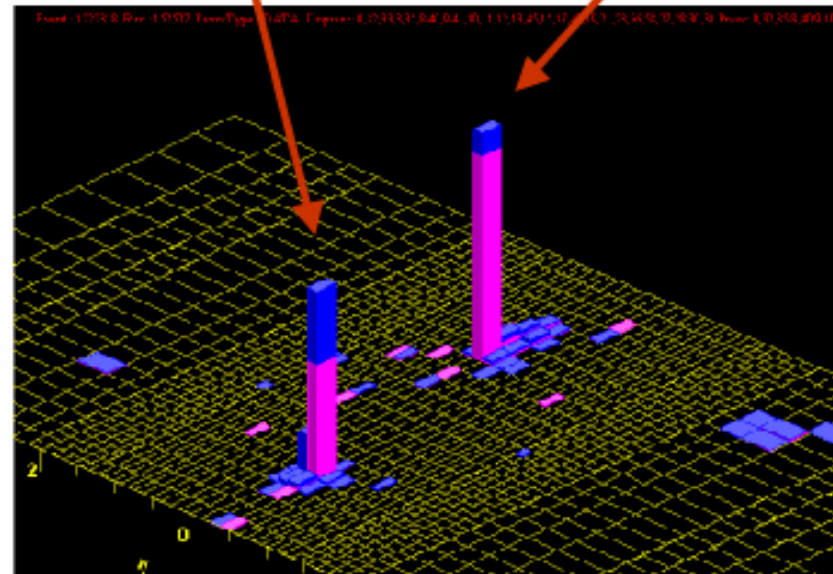
Inclusive Jet Production

- Nowhere is the increase in center-of-mass energy more appreciated



J2 $E_T = 633 \text{ GeV (corr)}$
 546 GeV (raw)
 J2 $\eta = -0.30 \text{ (detector)}$
 $= -0.19 \text{ (correct } z)$

J1 $E_T = 666 \text{ GeV (corr)}$
 583 GeV (raw)
 J1 $\eta = 0.31 \text{ (detector)}$
 $= 0.43 \text{ (correct } z)$



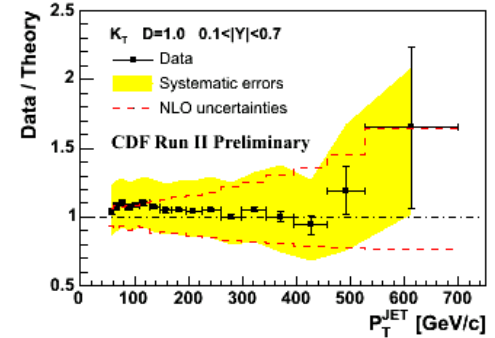
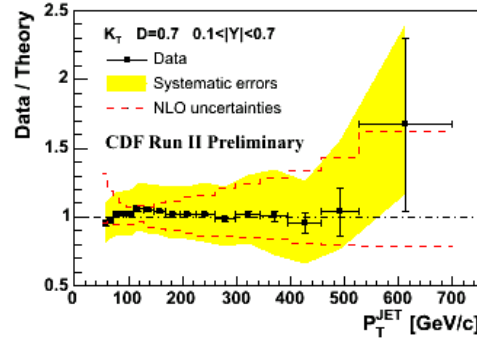
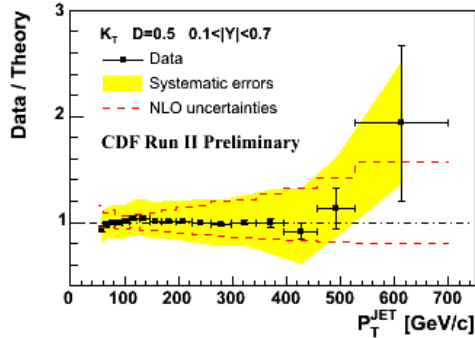
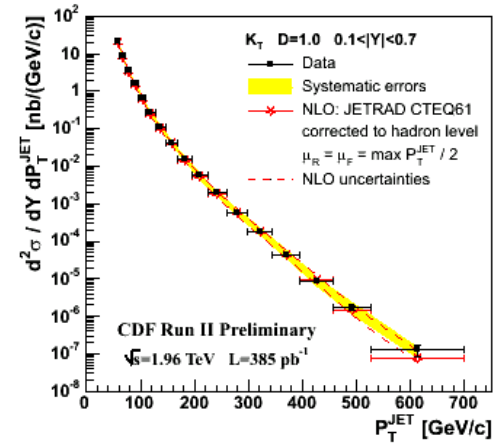
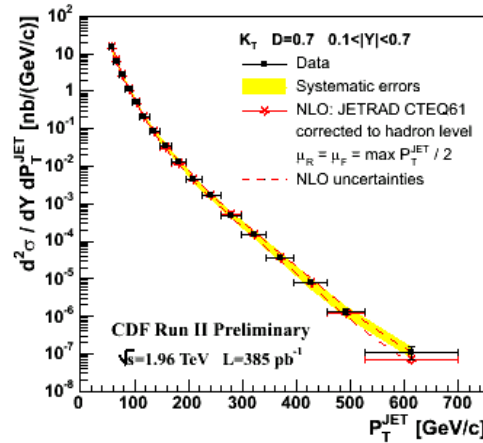
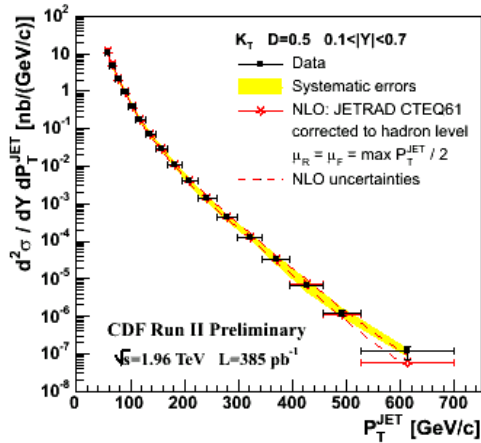
CDF Run 2 Preliminary

CDF: k_T jet cross section results

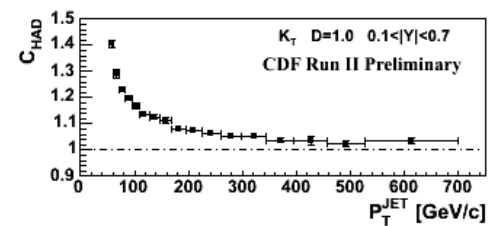
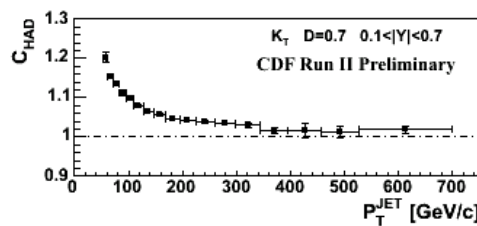
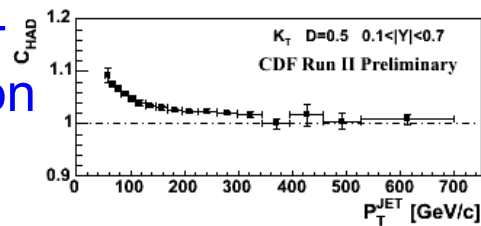
$$d_{ij} = \min(P_{T,i}^2, P_{T,j}^2) \frac{\Delta R^2}{D^2}$$

$$d_i = (P_{T,i})^2$$

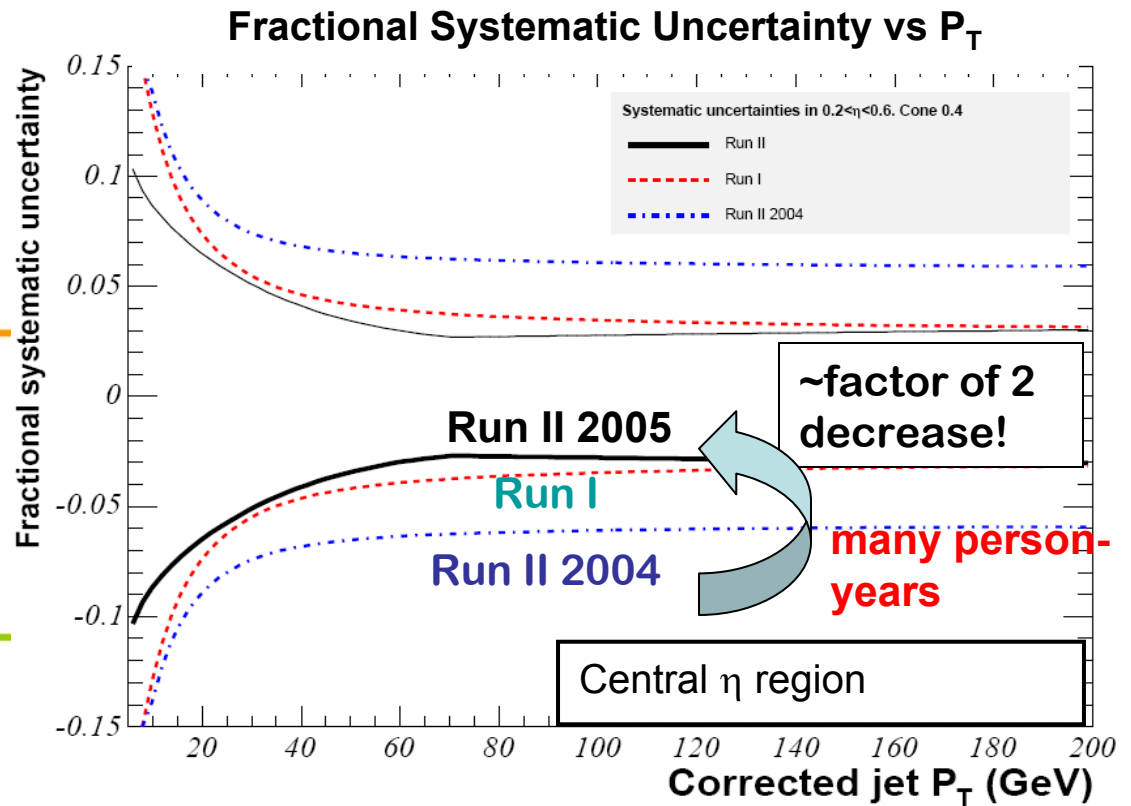
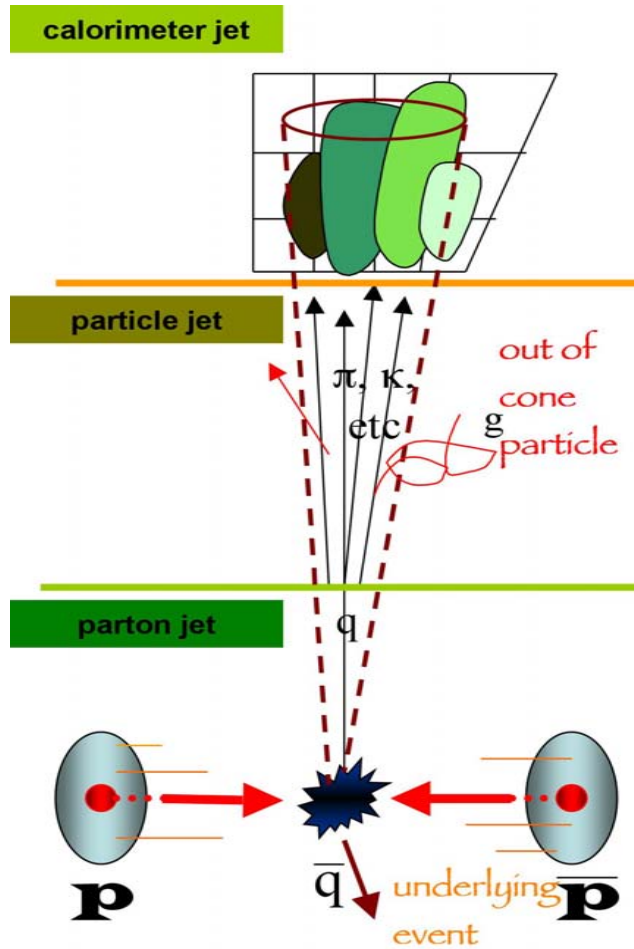
k_T algorithm
seems to
work well
at a hadron
collider



underlying +
hadronization
correction



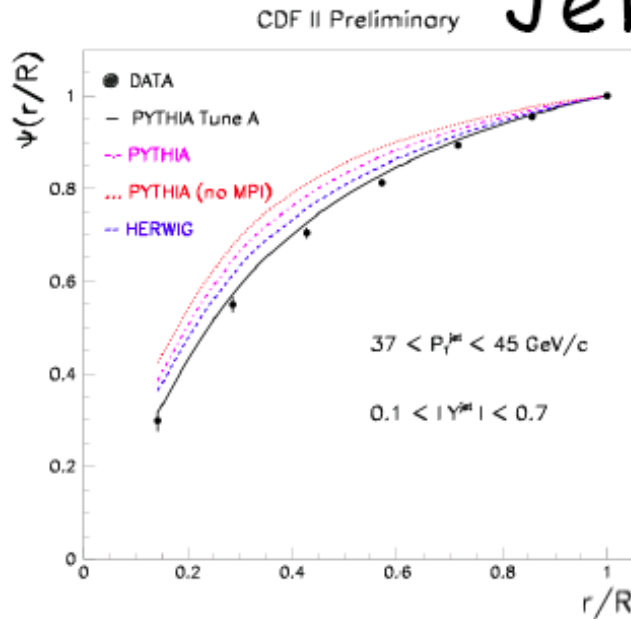
CDF Jet Energy Scale: from Run-1 to Run-2



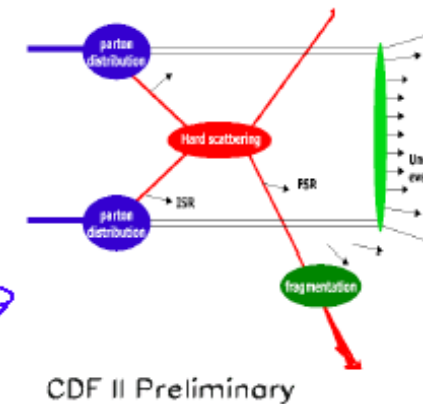
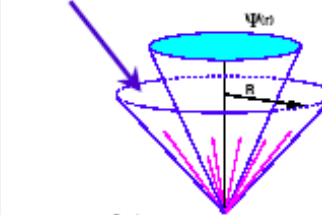
have to correct calorimeter energy depositions for detector, algorithm and physics effects to obtain “true” jet energy

Jet Fragmentation

Jet shapes



$1 - \Psi(r)$



- PYTHIA Tune A describes the data (enhanced ISR + MPI tuning)
- PYTHIA default too narrow
- MPI are important at low P_T
- HERWIG too narrow at low P_T

We know how to model the UE at 2 TeV (at least for QCD jet processes)

